

5/11/02

High Speed Civil Transport (HSCT) Isolated Nacelle Transonic Boattail Drag Study and Results Using Computational Fluid Dynamics (CFD)

Anthony C. Midea
NASA Lewis Research Center
Cleveland, OH 44135

Thomas Austin
McDonnell Douglas Aerospace
Long Beach, CA 90807

S. Paul Pao
NASA Langley Research Center
Hampton, VA 23681

James R. DeBonis
NASA Lewis Research Center
Cleveland, OH 44135

Mori Mani
McDonnell Douglas Aerospace
St. Louis, MO 63166

Nozzle boattail drag is significant for the High Speed Civil Transport (HSCT) and can be as high as 25% of the overall propulsion system thrust at transonic conditions. Thus, nozzle boattail drag has the potential to create a thrust-drag pinch and can reduce HSCT aircraft aerodynamic efficiencies at transonic operating conditions. In order to accurately predict HSCT performance, it is imperative that nozzle boattail drag be accurately predicted.

Previous methods to predict HSCT nozzle boattail drag were suspect in the transonic regime. In addition, previous prediction methods were unable to account for complex nozzle geometry and were not flexible enough for engine cycle trade studies. A computational fluid dynamics (CFD) effort was conducted by NASA and McDonnell Douglas to evaluate the magnitude and characteristics of HSCT nozzle boattail drag at transonic conditions. A team of engineers used various CFD codes and provided consistent, accurate boattail drag coefficient predictions for a family of HSCT nozzle configurations. The CFD results were incorporated into a nozzle drag database that encompassed the entire HSCT flight regime and provided the basis for an accurate and flexible prediction methodology.

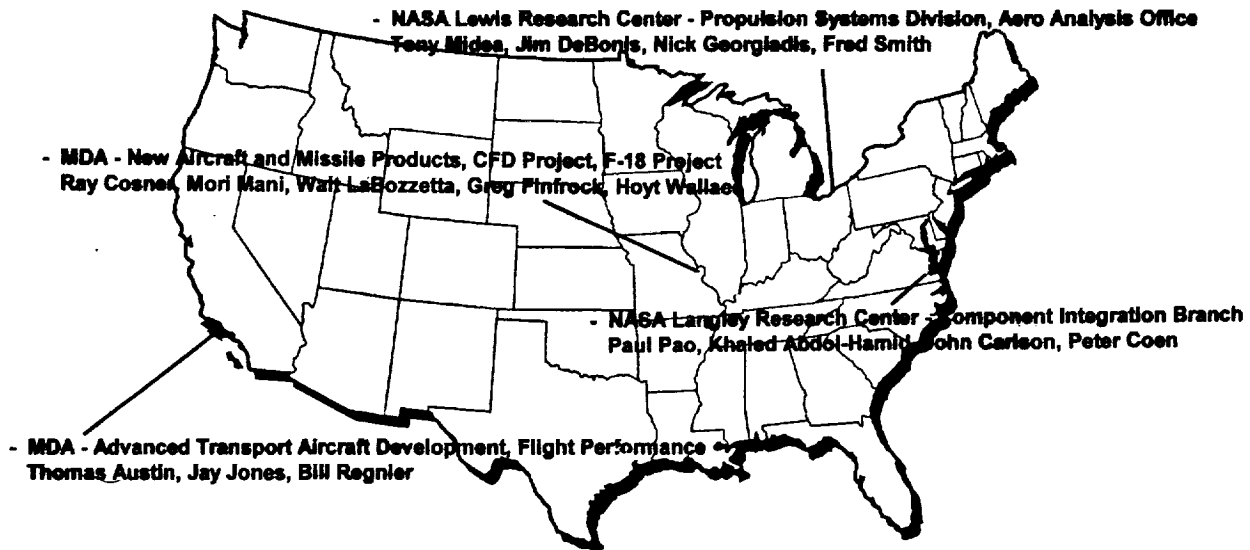


Nozzle boattail drag is caused by the generation of shock wave systems and regions of boundary layer flow separation on the nozzle external boattail surfaces. The shock wave systems and flow separation are due to the effects of the local flow field over the nacelle afterbody geometric curvature, and these effects yield a peak in nozzle boattail drag coefficient at transonic conditions. For the High Speed Civil Transport (HSCT), nozzle boattail drag is significant in the transonic flight regime, and can be as high as 25% of the overall propulsion system thrust. Thus, nozzle boattail drag has the potential to create a thrust-drag pinch and can reduce HSCT aircraft aerodynamic efficiencies at transonic operating conditions (Mach 0.95 to Mach 1.1). HSCT vehicle sizing and mission performance can be significantly impacted by transonic nozzle boattail drag predictions. In order to accurately predict HSCT performance, it is imperative that nozzle boattail drag be accurately predicted.

Cooperating Teams

o Investigation Coordinated by McDonnell Douglas (MDA)

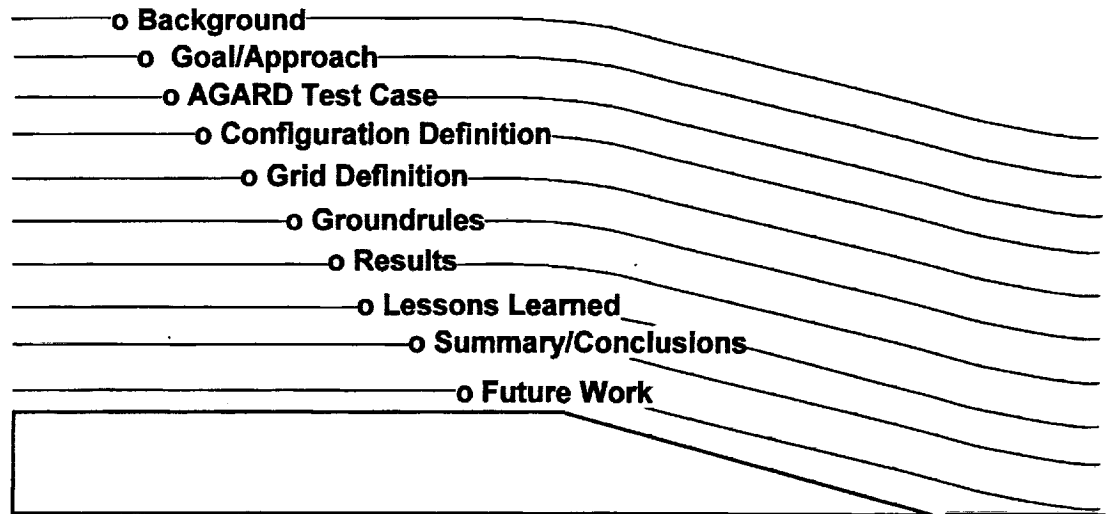
o Funded Internally by Four Participating Teams



o Working Period: August 16, 1994 to March 2, 1995

Four teams of analysts were involved in the CFD study; NASA Lewis Research Center - LeRC (Propulsion Systems Division, Aerospace Analysis Office), NASA Langley Research Center - LaRC (Component Integration Branch), McDonnell Douglas Aerospace - Advanced Transport Aircraft Development (ATAD) and New Aircraft and Missile Products (NAMP). Each team participated in the study with unique flow solvers, which will be described later. In addition, all work was funded internally by each of the participating teams, respectively. The study began August 16, 1994 and was completed on March 2, 1995.

Outline



Background

- o **Equivalent Axisymmetric Area Method was Previous Method**
- o **Previous Boattail Drag Method Inadequate for Detailed HSR Design Studies**
- o **Based on Empirical Axisymmetric Nozzle Data**
- o **Axi Nozzle Data Updated for 2D Nozzles Using Linear Theory**
- o **Transonic Data Suspect at Large Boattail Angles Due to Boundary Layer Separation Effects**
- o **Nozzle Approximated Using Simple Geometry**
 - **3D Effects Ignored**
 - **Detailed Design Analysis Not Possible**
- o **Method Not Flexible Enough For Engine Cycle Trade Studies**
 - **Sidewalls and Radius of Curvature Not Accounted For**
- o **Dovetail Isolated CFD Study Results with Integrated Mean Slope (IMS) Database Update to Create Accurate Boattail Drag Prediction Method**

Prior to March 1995, HSCT nozzle boattail drag was predicted using an equivalent axisymmetric area method. This method was formulated by NASA and industry and assumed that nozzle geometry could be approximated with simple area ratio and length data. For axisymmetric nozzles, the method was based on an empirical axisymmetric nozzle database, (Silhan & Cabbage data).

For non-axisymmetric nozzles, the tables were updated, but the method of calculating boattail angle remained the same. In effect, the non-axisymmetric nozzle boattail angle was calculated assuming equivalent axisymmetric areas. The tables of empirical axisymmetric data were updated to represent non-axisymmetric nozzles using drag deltas between axi and non-axi nozzle types obtained from a parametric linear theory analysis. This approximation was adequate for the preliminary design phase of the HSCT project, but proved to be inadequate for detailed design studies.

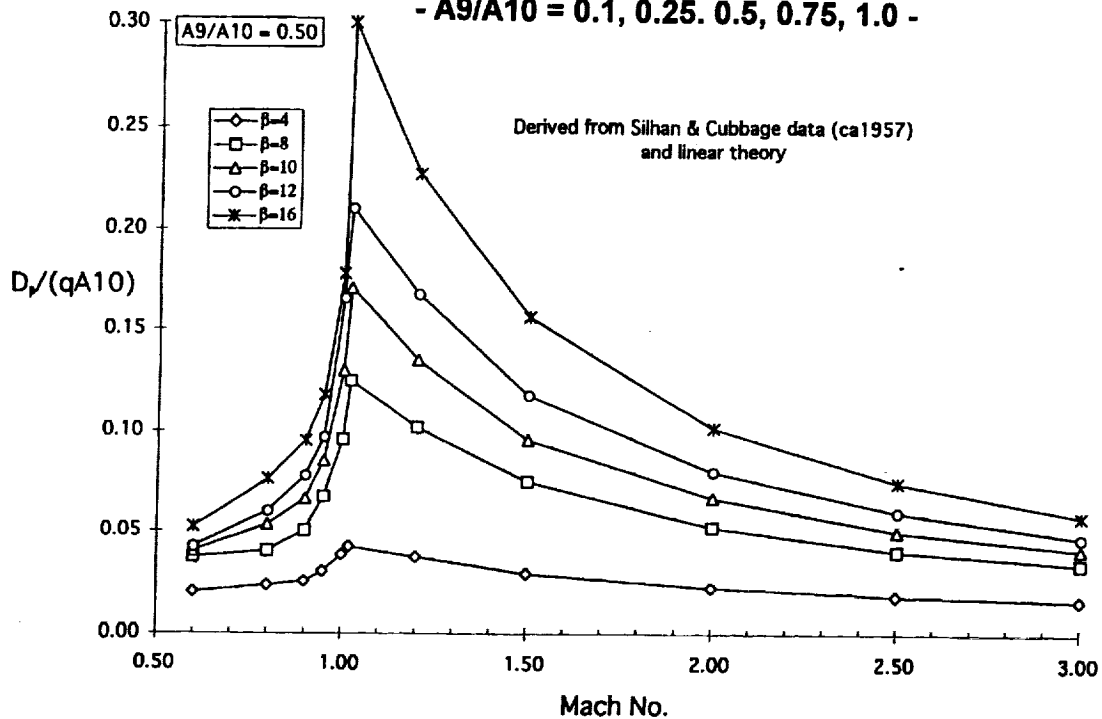
Much of the HSCT propulsion system activity focused on non-axisymmetric nozzles. Detailed design studies of non-axisymmetric nozzles exposed various deficiencies with the previous boattail drag method. The original axisymmetric database yielded little transonic drag information, and the curves were approximate from Mach 0.9 to 1.1. Typically, boattail drag coefficient peaks in this Mach regime at all altitudes, thus, it was possible that the peak boattail drag coefficients and transonic drag rise characteristics were not being approximated correctly. In addition, the previous boattail drag method used a simple method to approximate nozzle geometry that ignored nozzle sidewalls, radius of curvature, 3-D effects and other detailed design characteristics.

In summary, the previous nozzle boattail drag prediction methodology for non-axisymmetric nozzles was not accurate in the transonic flight regime, and was not flexible enough to capture the effects on boattail drag due to detailed three-dimensional geometry changes. A new method was required to accurately predict boattail drag throughout the flight regime in a timely fashion. The approach taken was to employ an Integral Mean Slope (IMS) method using an upgraded nozzle boattail drag database. In addition, a concurrent activity was to be conducted employing advanced Navier-Stokes computational fluid dynamics (CFD) methods to update and substantiate the transonic portion of the updated nozzle drag database.

LeRC/PW Boattail Drag Tables

Rectangular (2D) Nozzles

- $A_9/A_{10} = 0.1, 0.25, 0.5, 0.75, 1.0$ -

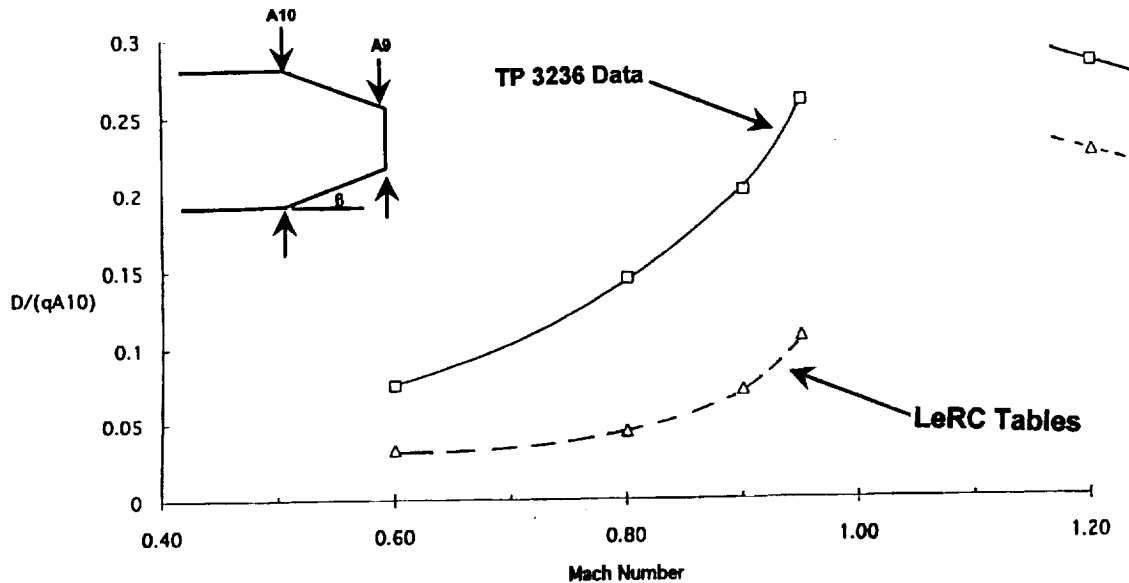


The previous method used a database based on empirical data. The empirical axisymmetric nozzle data were plotted and curve fitted to provide a continuous data set. Plots of nozzle boattail drag as a function of Mach number were made for constant area ratio with boattail flap angle as the independent variable. The boattail drag coefficient values in the database are a function of Mach number with boattail flap angle as the independent variable. The figure shows an example of one of these plots for the non-axisymmetric nozzle database with a constant nozzle area ratio (A_9/A_{10}) of 0.5. Similar plots exist for area ratios of 0.1, 0.25, 0.75 and 1.0. Nozzle height ratio was defined as the nozzle exit height (h_9) divided by the maximum nozzle external height (h_{10}), or h_9/h_{10} . Nozzle area ratio was defined as nozzle exit area (A_9) divided by maximum nozzle external area (A_{10}), or A_9/A_{10} . Boattail flap angle was calculated using A_9 , A_{10} and the divergent flap external length between A_9 and A_{10} . Nozzle boattail drag was then determined using the five empirical tables and the following inputs; (Mach number, A_9/A_{10} , and β).

Background

- Previous Method Comparison to Test Data - (Transonic 2D Nozzle Drag Characteristics)

NASA LaRC TP 3236, Configuration 9, No Plume
RC/DM = 0.40, $\beta = 17.9^\circ$, $A_9/A_{10} = 0.14$
Equivalent axis $\beta_{eq} = 12.65^\circ$

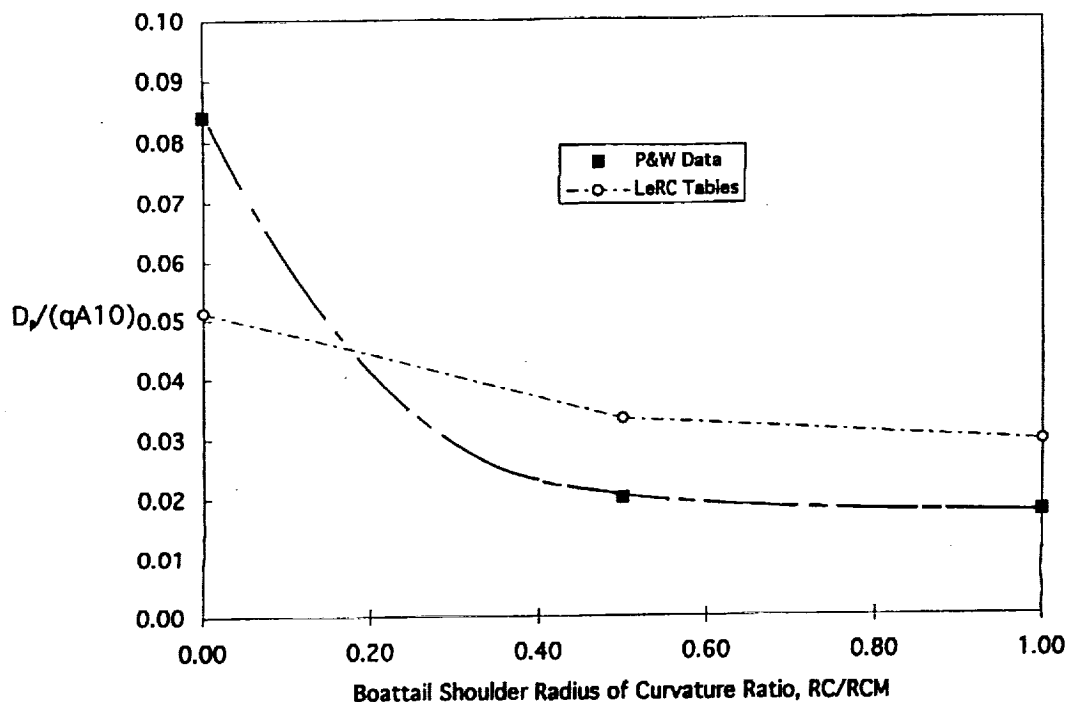


The figure shows a comparison of the previous non-axisymmetric method with experimental boattail drag data for a non-axisymmetric nozzle. The nozzle has a 17.9 degree boattail angle and an area ratio of 0.14. This comparison shows that the previous method significantly underpredicts transonic boattail drag coefficient for this specific nozzle configuration. Comparisons of various non-axisymmetric nozzles with experimental data were made using the previous method, and the results were consistent with the trends shown in this figure.

Comparison of Nozzle Drag Data w/Previous Method

- 2D Nozzle, $A_9/A_{10}=0.25$, $\beta = 16$ deg -

$M = 0.9$



This figure shows a comparison between the previous non-axisymmetric method with experimental boattail drag data for a non-axisymmetric nozzle. This comparison shows that the previous method cannot accurately approximate nozzle boattail drag trends due to detailed design geometry changes, such as changes in nozzle radius of curvature ratio (RC/RCM). Nozzle radius of curvature ratio is essentially a measure of the smoothness of the area distribution of the nozzle. A RC/RCM=0.0 indicates a nozzle with a sharp angle at the boattail flap hinge line. A RC/RCM=1.0 indicates a nozzle with no discontinuities in the area distribution from the nozzle maximum area to the nozzle exit. Because of its inability to characterize detailed nozzle geometry changes, the previous method was not flexible enough to conduct engine cycle and nozzle trade studies that are required to differentiate between detailed designs and perform component downselect activities.

Goal/Approach

- o Goal: Develop Accurate Method to Provide Timely Boattail Drag Calculations for 2D M/E HSCT Nozzles by March 1995 (Nozzle Downselect Studies)**
- o Impetus:**
 - HSCT Nozzle Boattail Drag as High as 25% of Transonic Thrust**
 - HSCT Nozzles Complex 3D Configuration**
 - Limited Data Available for Non-axisymmetric Nozzles**
- o Approach**
 - Employ Advanced N-S CFD Methods to Update/Substantiate Database**
 - Update MDA IMS Database Using CFD Results and Non-axi Nozzle Data**
 - Analyze Interference Effects of Installed Nozzles/Nacelle (Phase II)**

Based on previous experience, transonic nozzle drag data would be difficult to obtain. The approach taken to achieve the above goal was to employ advanced Navier-Stokes computational fluid dynamics (CFD) methods to obtain accurate and reliable transonic nozzle drag coefficient data. In addition, a concurrent activity was initiated to implement an Integral Mean Slope (IMS) method using an updated nozzle boattail drag coefficient database to predict boattail drag. The IMS method is widely used and offers a detailed representation of the nozzle geometry in a timely fashion. The nozzle boattail drag database was to be updated using all known wind tunnel and flight test nozzle data for HSCT type nozzles. The transonic CFD boattail drag coefficient predictions were to be used to update and substantiate the IMS transonic nozzle boattail drag coefficient database. The new method was required in March 1995 for use in the nozzle downselect studies.

IMS Update Study Approach

- o Update IMS Database (MDA-NAMP w/MDA-ATAD IRAD)**
- o Base Update on Isolated Nozzles**
 - Applicable to Low Interference Nacelles**
 - Applicable for Sharp-Cornered to Full Radius Boattail Shoulders**
- o Updated IMS Results Presented to HSR Community on 1 March 1995**
- o CFD Results to Substantiate IMS Update**

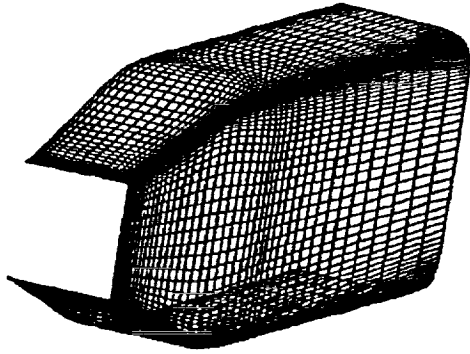
The IMS database update activity was performance by MDA with internal funding. The update was based on isolated non-axisymmetric nozzles, and was applicable for low interference nacelles, and for a full range of radius of curvature ratios. The updated IMS results were presented to the HSR community in March 1995.

CFD Study Approach

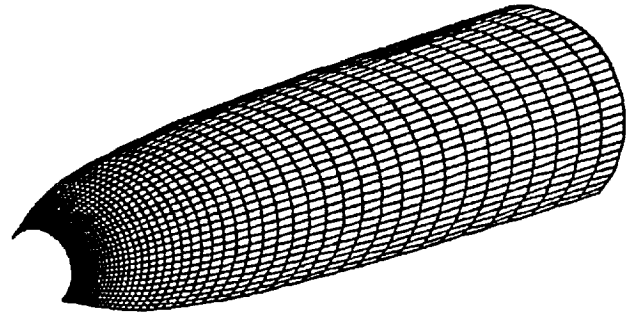
- o Validate All Codes by Comparison with AGARD 17 Axi and 2D Nozzle Test Performance Data (NASTD & PAB3D Previously Validated, NPARC3D Validated as Part of This Study)**
 - NASTD (McDonnell Douglas Aerospace)**
 - PAB3D (NASA Langley Research Center)**
 - NPARC3D (NASA Lewis Research Center)**
- o Generate 3D Navier-Stokes CFD Solutions of HSCT MFTF 3765-100**
 - Parametric Study of Nozzle Boattail Flap Angle and Area Ratio**
 - Transonic Mach Numbers (0.95, 1.1 & 1.2)**
 - Reference Cruise Geometry at Mach 2.4**
 - $A_9/A_{10}=0.5$, Boattail Flap Angle=16 deg Test Case for All Participants For HSCT Explicit Code Validation**
- o Use CFD Results of Representative HSCT Nacelle Configurations to Provide Delta Cds at Transonic Conditions**

Three unique flow solvers were used in this study; NASTD (MDA), PAB3D (NASA LaRC) and NPARC (NASA LeRC). The first step in the approach was to validate these unique flow solvers for a representative configuration using well documented and tested nozzles from the Advisory Group for Aerospace Research and Development (AGARD) Working Group #17. After successful completion of this validation step, the three codes would be used to generate solutions for a series of HSCT specific nozzle configurations. A parametric study of nozzle boattail flap angles (12-20 degrees), area ratios ($A_9/A_{10}=0.2-0.5$), and Mach numbers (0.95-1.1) was to be conducted. The $A_9/A_{10}=0.5$, 16 degree boattail angle case was selected by team members to be a common case that all members would solve to provide a second validation. The final solutions to all of the configurations was then to be used to update and substantiate the IMS database.

AGARD 17 Test Case Nozzles



2D B.4 Nozzle



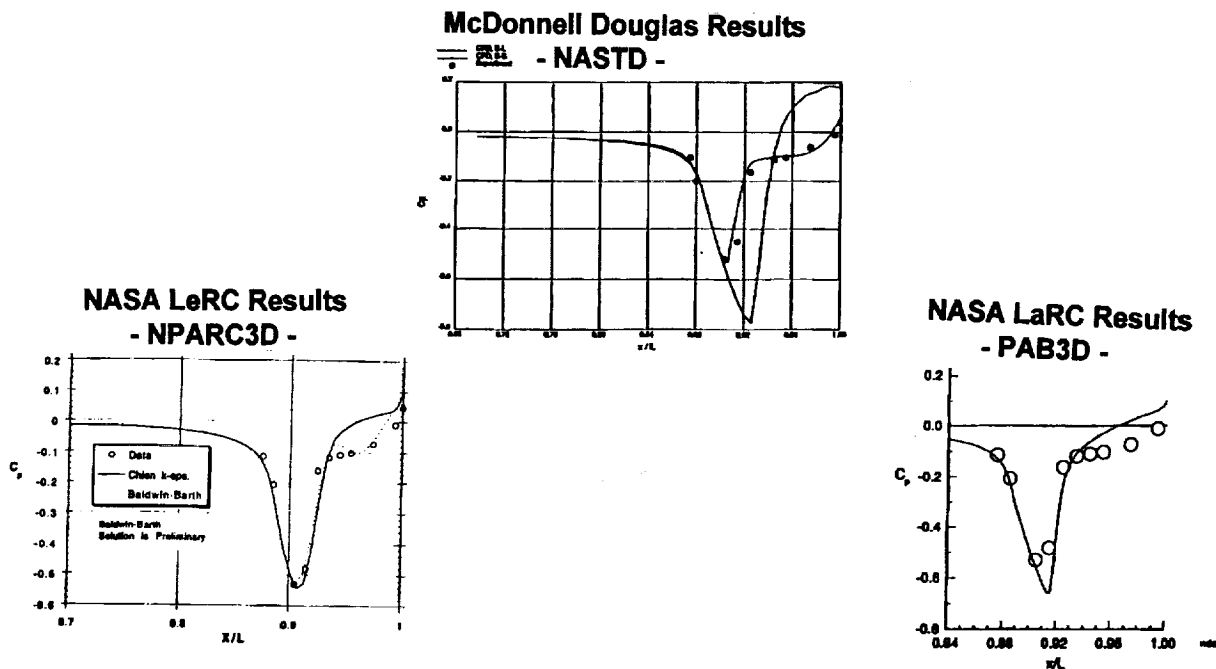
Axisymmetric B.1 Nozzle

Two of the nozzles from the AGARD Working Group #17 tests that were used for flow solver validation are shown in the figure. The B.4 nozzle is a two-dimensional nozzle without sidewalls. The B.1 nozzle is an axisymmetric nozzle. Three validation cases were executed at Mach 0.94 including; (a) axisymmetric nozzle (B.1), attached flow, (b) axisymmetric nozzle (B.1), separated flow, and (c) non-axisymmetric nozzle (B.4), separated flow. In general, the axisymmetric nozzle cases required significantly less computational resources than the non-axisymmetric case, and yielded consistent results for all of the CFD codes. While the axisymmetric cases were required for validation, the focus of this effort was placed upon the non-axisymmetric case, because this case closely resembled an HSCT type nozzle.

AGARD 17 Test Case Comparison Results

- B.4.2 2D C-D Nozzle -

Mach 0.94, NPR=4, Centerline Pressure Comparison

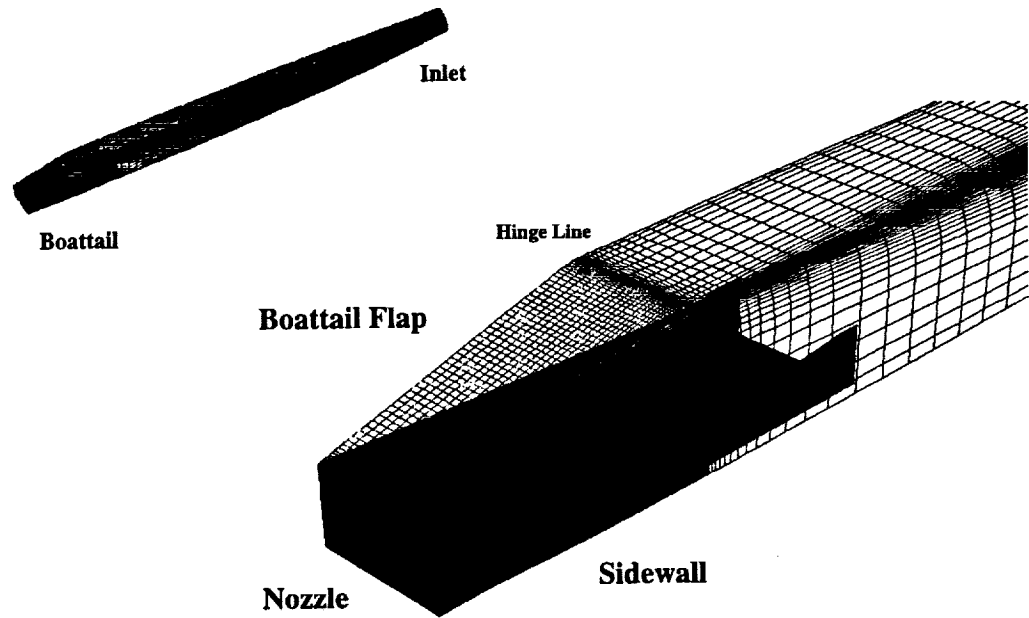


The B.4 nozzle closely approximated an HSCT type nozzle because it was a two-dimensional nozzle that experienced separated flow at transonic speeds. Although the B.4 did not have sidewalls, the nozzle still provided an opportunity to gain insight on how well the flow solvers could predict nozzle boattail pressure coefficient, and thus nozzle boattail drag.

The figure shows a comparison between nozzle B.4 centerline pressure coefficient test results and CFD predictions. Three plots are shown that graphically compare each of the three CFD codes involved in this study. The plots are set up to compare pressure coefficient as a function of non-dimensional distance (x/L) along the centerline, and the experimental results are identical for all three plots. From the NASTD plot, the conclusion can be drawn that NASTD with the Baldwin-Barth turbulence model accurately predicts the absolute values of experimental data as well as the trends with non-dimensional centerline distance. The NPARC plot using the Baldwin-Barth turbulence model also shows excellent agreement with the experimental data and closely resembles the NASTD prediction. In addition, the PAB3D plot exhibits excellent agreement with the experimental data. Note that PAB3D slightly overpredicts pressure coefficient near the trailing edge of the nozzle, and this could lead to a slight underprediction of drag coefficient for this specific case using a two equation, linear k-e turbulence model.

The results of this figure, coupled with the excellent agreement between CFD and experimental results for the axisymmetric cases (not shown explicitly here), indicate that NASTD, NPARC and PAB3D are clearly capable of accurately predicting pressure coefficient distributions for HSCT type nozzles in the transonic flight regime. Thus, the CFD codes are validated with experimental pressure coefficient data. The next step was to ensure that the codes compared favorably with each other using the HSCT DSM nozzle.

Typical Isolated HSR Nacelle Configuration: Boattail Drag Study



The figure shows a typical isolated HSCT nacelle configuration used in the CFD study. The nacelle is full scale, and includes inlet, engine and nozzle components.

Configuration Definition: Inlet & Nozzle

Inlet

- o Generic Axi Inlet with Mass Flow Ratio Equal to 1.0
- o Upstream Inviscid Streamtube Modeled

Nozzle

- o Geometry Scaled to Full Scale MFTF 3765-100 Engine
- o Sidewalls Modeled
- o Corners Rounded with 8 In Radius Corner Per 3765-100 Design
- o Sharp Transition At External Flap Hinge Line (Radius of Curvature Ratio, $RC/RCM=0.0$)
- o Internal Nozzle Plenum Chamber, Throat, Diffuser and Exit Modeled
- o Internal Nozzle Angle Fixed at 1.5 deg to Maintain Constant Exit Flow Divergence Angle
- o Boattail Flap Angles (12, 16 and 20 deg) Chosen to Encompass Actual Transonic Boattail Angle = 13.68 deg
- o Nozzle Height Ratios (0.2 and 0.5) Chosen to Encompass Actual Transonic Area Ratios = 0.274 to 0.320

The inlet was modeled as a generic, axisymmetric inlet with a mass flow of 1.0 (no spillage). Also, the upstream inviscid streamtube was modeled. The nozzle geometry was based on the latest HSCT non-axisymmetric nozzle design (Downstream Mixer (DSM) mixer/ejector nozzle). The nozzle geometry was scaled to the full scale mixed flow turbofan (MFTF) size, which is described below. The nozzle sidewalls were modeled, and the corners of the nozzle were rounded with 8 inch radii to match the DSM design. The nozzle was designed with a sharp transition at the external flap hinge line, thus representing a radius of curvature ratio (RC/RCM) of zero. Internally, the nozzle plenum chamber, throat, diffuser and exit were modeled, and the nozzle was modeled with hot gas. The internal nozzle angle was fixed at 1.5 degrees to maintain constant exit flow divergence angle.

A family of nozzles was studied at three Mach numbers; $M=0.95$, 1.1 and 1.2. Various nozzle boattail angle and nozzle area ratio values were modeled to represent a wide array of nozzle configurations. Boattail angles of 12, 16 and 20 degrees were chosen to encompass the range of boattail angles expected at transonic conditions. Also, nozzle height ratios of 0.2 and 0.5 were chosen to encompass the range of area ratios expected at transonic conditions. The height ratios correspond to area ratios of 0.187 and 0.467, respectively, which were rounded to 0.2 and 0.5, respectively, for convenience. The matrix of nozzle configurations studied is described later.

Configuration Definition: Engine Cycle

- o **3765-100 Best Represented HSCT Cycle at Time of Study**
 - **Mixed Flow Turbofan Designed by PW/GE**
 - **Demonstrated Feasible HSCT Aircraft Performance**
 - **BPR = 0.622 (sea level static)**
- o **Datapak A8, PT8, and TT8 Used to Define Plenum Conditions For Internal Nozzle Flow Modelling**

At the time of this study, the 3765-100 MFTF was the leading engine cycle candidate. This cycle is a mixed flow turbofan, designed by Pratt & Whitney and General Electric, and has a fan pressure ratio of 3.7, and airflow lapse rate of 65% and requires 900 lb/s of corrected airflow at sea level static conditions. The airflow lapse rate is simply the percentage of cycle flow at cruise versus takeoff conditions. For this cycle, the cycle required airflow at cruise is 65% of the required takeoff airflow. This cycle has a bypass ratio of 0.622, and has demonstrated feasible HSCT aircraft performance. Area and pressure data were obtained from the engine company datapack to define the nozzle plenum conditions; (throat area, pressure and temperature). Therefore, the hot gas flow should closely approximate the actual 3765 MFTF cycle installed with a DSM type nozzle.

Configuration Definition: Nacelle

- o Full Scale Nacelle Based on PW/GE 3765-100 MFTF Design**
- o Isolated Nacelle Modeled**
- o Wing Installation Effects Not Modeled**
- o One-Quarter of Nacelle Modeled**
 - Assumed Horizontal and Vertical Streamwise Symmetry**
 - Reduced Computational Resources**
- o Forebody Nacelle Geometry Identical to Actual 3765-100 MFTF**

The inlet, engine cycle and nozzle components were integrated, and a nacelle shape was chosen. The nacelle shape is axisymmetric at the inlet cowl lip, and continuously transitions from axisymmetric to non-axisymmetric ending at a non-axisymmetric (2D) shape at the external flap hinge line. From the hinge line aft to the nozzle exit, the nozzle is entirely non-axisymmetric. The nacelle was modeled as full scale and was based on the 3765-100 airflow requirements. This study only examined the isolated nacelle, and did not explore the effects of integrating the nacelle with a wing. Therefore, wing effects were not modeled. One-quarter of the nacelle was actually modeled with CFD grid, and horizontal and vertical streamwise symmetry were assumed. This saves considerable computational resources with no loss in accuracy of results.

CONFIGURATION RUN MATRIX

Configuration	A_9/A_{10}	Boattail	M_∞	Team
N0010	1.0	0°	0.95, 1.10, 1.20	NASA Langley
N1202	0.2	12°	0.95, 1.10, 1.20	NASA Lewis
N2002	0.2	20°	0.95, 1.10, 1.20	NASA Langley
N1205	0.5	12°	0.95, 1.10, 1.20	MDA-ATAD
N1605	0.5	16°	0.95, 1.10, 1.20	MDA-ATAD MDA-NAMP NASA Langley NASA Lewis
N2005	0.5	20°	0.95, 1.10, 1.20	MDA-NAMP

The configuration run matrix is shown in the figure. The N1605 configuration was the baseline configuration that was studied by all four teams. The 16 in the configuration designation represents the boattail angle in degrees, and the 05 represents an area ratio of 0.5. Each team was responsible for the N1605 configuration and one other configuration. Because each configuration was to be run at three Mach numbers (0.95, 1.1 and 1.2), this represented a total of 6 CFD runs per team member. NASA LaRC was also responsible for the N0010 configuration, which contributed three additional CFD runs and were critical for the purposes of this study. The N0010 configuration represents a nozzle with zero boattail angle, and an area ratio of 1.0. In this study, only the drag due to the nozzle is of interest, thus, the drag of the N0010 nacelle must be subtracted from the drag of all the other CFD runs (at the respective Mach number) to obtain the nozzle specific drag at any given condition.

NACELLE CONFIGURATIONS

CASE	M_∞	A_8/A_9	A_9/A_{10}	Boattail Angle	Equivalent Boattail Angle	Boattail Flap Length
N0010	0.95	0.709	1.0	0°	0.00°	174.4 in.
	1.10	0.651				
	1.20	0.606				
N1202	0.95	0.709	0.2	12°	8.82°	174.4 in.
	1.10	0.651				
	1.20	0.606				
N2002	0.95	0.709	0.2	20°	14.46°	107.1 in.
	1.10	0.651				
	1.20	0.606				
N1205	0.95	0.709	0.5	12°	7.60°	107.0 in.
	1.10	0.651				
	1.20	0.606				
N1605	0.95	0.709	0.5	16°	9.94°	82.0 in.
	1.10	0.651				
	1.20	0.606				
N2005	0.95	0.709	0.5	20°	12.51°	65.3 in.
	1.10	0.651				
	1.20	0.606				

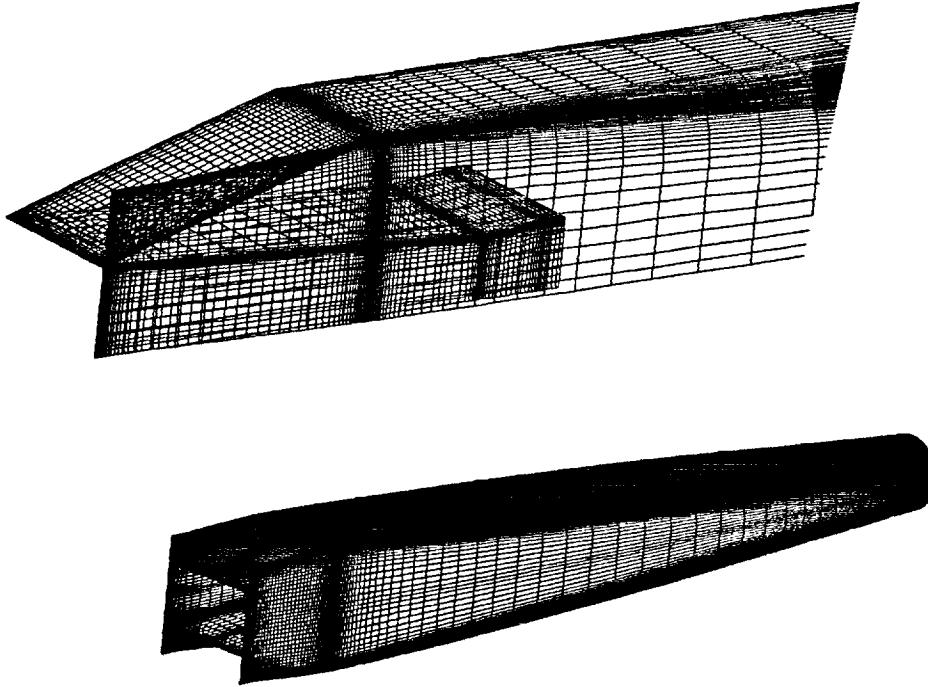
Additional detailed nacelle information is presented in the figure. The nozzle throat to exit area ratio (A_8/A_9), boattail angle, equivalent boattail angle, and flap length are given. The equivalent boattail angle is the equivalent axisymmetric nozzle boattail angle, and is defined by the nozzle area ratio and boattail flap length.

CFD Grid Definition

- o **MDA Defined Grid Topologies and Generated Initial Grids**
- o **NASA LaRC Optimized the Final Surface and Volume Grids**
- o **3D, Structured, Patched, Viscous, Multi-Block CFD Grids**
- o **External and Internal Surfaces Modeled as Viscous Surfaces**
- o **Viscous Grid Generated to Model Free Shear Layers in Nozzle Exhaust**
- o **Nozzle Sidewall Trailing Edge Modeled with Zero Thickness**
- o **All Zones Point-Matched Except for Upstream and Far-Field Zones**
- o **Nozzle Plenum Chamber Configuration Based on AGARD B.4 Config**
- o **Approx. 1.5 Million Grid Points Per Configuration**

All grid topologies and initial grids were defined by MDA for this study. NASA LaRC optimized the final surface and volume grids for use by all teams. The grids were 3D, structured, patched, viscous, multi-block grids. The external and internal surfaces were modeled as viscous surfaces, and a viscous grid was generated to model free shear layers in the nozzle exhaust. The nozzle sidewall trailing edge was modeled with zero thickness, and the sidewalls ended at the trailing edge of the external flaps. All zones were point matched except for upstream and far-field zones. The nozzle plenum chamber configuration was based on the AGARD non-axisymmetric nozzle configuration. A total of approximately 1.5 million grid points were used for each individual configuration. A non-dimensional viscous height of $y^+ = 2$ was employed to define the first grid cell spacing off the viscous surfaces.

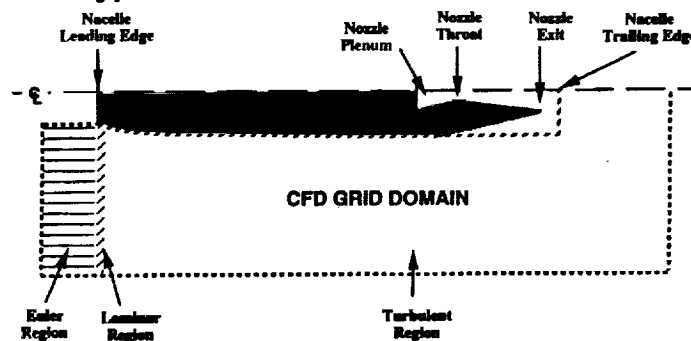
Nacelle CFD Grid



This figure shows a typical nacelle grid for a full nacelle and a side view of a representative quarter nacelle complete with the internal and external nozzle characteristics.

Groundrules

- o **CFD Convergence Criteria**
 - Converged Boattail Pressure Drag Force Levels
 - Converged Internal Nozzle Massflow Rate Levels
 - Reduction of L2 Residuals in Boattail Region by 3 Orders of Mag
- o **Boattail Drag Computations**
 - Pressure Drag on Boattail Defined as the Integration of $(P - P_{inf})$ Over Respective Nacelle Surfaces
 - Skin Friction Drag Not Computed
 - Delta Drag Coefficient Computed Using Nacelle Reference Config (Cruise Configuration)
- o **CFD Flow Type Definition**



The CFD convergence criteria were as follows. The boattail pressure drag force level must converge within 0.1% of the total drag force. In addition, the internal nozzle exit massflow rate level required convergence within 0.25% of the intake massflow rate, (e.g. conservation of mass). Finally, the L2 residuals must be reduced in the boattail flap region by three orders of magnitude. All three criteria must be met as a condition for a converged solution.

Nozzle boattail drag was computed using the predicted pressure distributions on the boattail surfaces. Integration of the pressure distributions over the respective nozzle boattail surfaces yielded the nozzle boattail drag results. The surfaces used in the integration included the nozzle flaps and nozzle sidewalls. Skin friction drag was not computed. Because the nozzle boattail drag for each of the configurations was influenced by the presence of the nacelle forward of the nacelle maximum area, the reference nacelle drag (configuration N0010) was subtracted from the actual boattail drag for each configuration. The reference nacelle had zero boattail angle.

The CFD flow type definition groundrules are shown in the figure. An Euler region was defined just prior to the nacelle configuration to simulate the captured streamtube, and a small laminar region was defined at the nacelle leading edge to simulate transition. The problems were set up in this fashion to allow the flow solvers to begin the solution free of discontinuities. The remaining nacelle was modeled as a turbulent region.

COMPUTED NOZZLE BOATTAIL DRAG RESULTS

Configuration	Boattail	A_9/A_{10}	M_∞	$C_{d, \text{boattail}}$	$C_{d, \text{boattail}} \text{ [lb]}$	Team	CFD Code
N1202	12	0.2	0.95	0.1087	550.0	NASA LeRC	PARC3D
N1202	12	0.2	1.10	0.1827	1238.8	NASA LeRC	PARC3D
N1202	12	0.2	1.20	0.1840	1484.7	NASA LeRC	PARC3D
N1205	12	0.5	0.90	0.0422	191.7	MDA-ATAD	NASTD
N1205	12	0.5	0.95	0.0501	253.5	MDA-ATAD	NASTD
N1205	12	0.5	1.10	0.0809	548.3	MDA-ATAD	NASTD
N1205	12	0.5	1.20	0.0985	794.7	MDA-ATAD	NASTD
N1605	16	0.5	0.90	0.0504	228.7	MDA-ATAD	NASTD
N1605	16	0.5	0.95	0.0678	342.9	MDA-ATAD	NASTD
N1605	16	0.5	1.10	0.1847	1252.7	MDA-ATAD	NASTD
N1605	16	0.5	1.20	0.1645	1327.6	MDA-ATAD	NASTD
N1605	16	0.5	0.95	0.1426	721.1	MDA-NAMP	NASTD
N1605	16	0.5	1.10	0.1969	1335.5	MDA-NAMP	NASTD
N1605	16	0.5	1.20	0.1802	1454.6	MDA-NAMP	NASTD
N1605	16	0.5	0.95	0.0939	474.9	NASA LaRC	PAB3D
N1605	16	0.5	1.10	0.2094	1419.9	NASA LaRC	PAB3D
N1605	16	0.5	1.20	0.1962	1583.6	NASA LaRC	PAB3D
N1605	16	0.5	0.95	0.1343	679.1	NASA LeRC	PARC3D
N1605	16	0.5	0.95	0.1284	649.4	NASA LeRC	PARC3D
N1605	16	0.5	1.10	0.2084	1413.5	NASA LeRC	PARC3D
N1605	16	0.5	1.20	0.1960	1581.8	NASA LeRC	PARC3D
N2002	20	0.2	0.95	0.1728	873.9	NASA LaRC	PAB3D
N2002	20	0.2	1.10	0.3759	2548.9	NASA LaRC	PAB3D
N2002	20	0.2	1.20	0.3594	2900.6	NASA LaRC	PAB3D
N2005	12	0.5	0.95	0.1707	863.2	MDA-NAMP	NASTD
N2005	12	0.5	1.10	0.2414	1637.2	MDA-NAMP	NASTD
N2005	12	0.5	1.20	0.2209	1782.6	MDA-NAMP	NASTD

The nozzle boattail drag CFD solutions are tabulated and summarized in this figure.

Mach Number Contours Along Centerline - 1605 Configuration, Mach 0.95 -

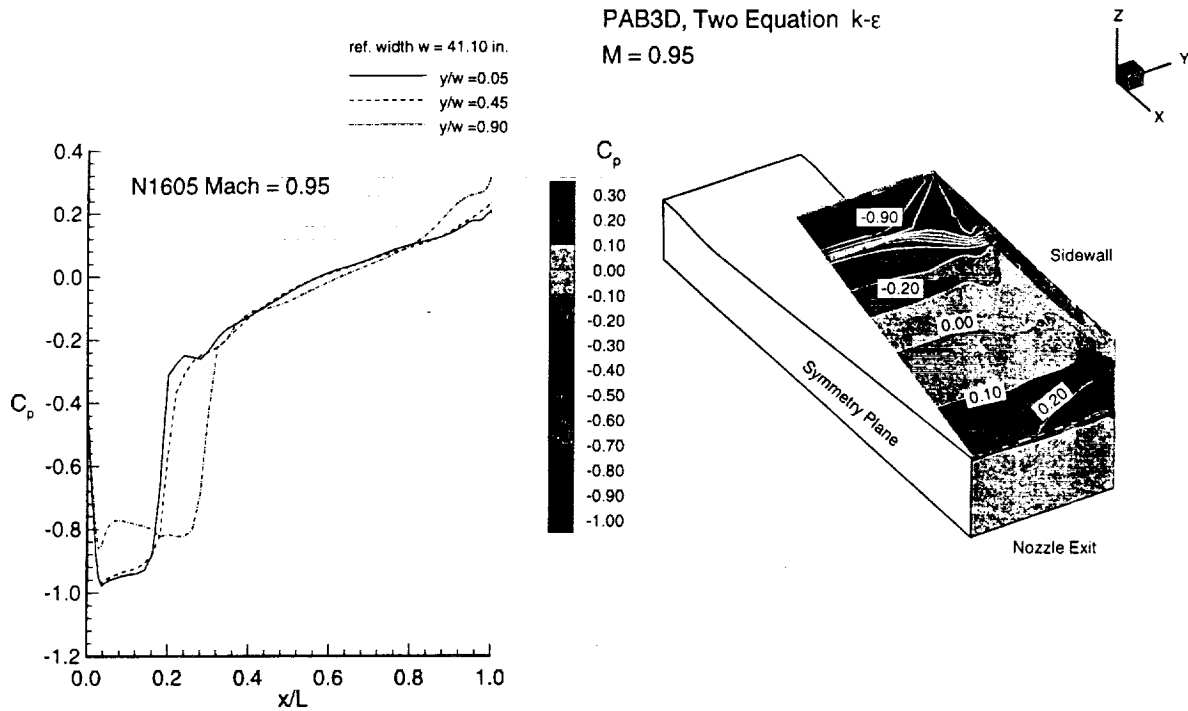


Prior to commencing the entire CFD study for all of the configurations, a baseline case was chosen to validate drag coefficient results between codes for an HSCT specific nozzle. The 16 degree boattail case with an 0.5 area ratio (1605) was chosen as the baseline case, primarily because this case effectively represented the median of the configuration with respect to boattail flap angle. This case was studied by all four teams, and is presented in detail on the following charts.

The figure shows the Mach number contours along the centerline of the top flap of the 1605 nozzle at Mach 0.95. The flow is uniform prior to the nozzle hinge line, and begins to expand at the nozzle flap hinge line. For this case, the external flow expands around the nozzle boattail flap hinge line and recompresses through a normal shock wave just downstream of the expansion wave. Significant separation from the afterbody surface occurs behind the normal shock wave, and the flow does not reattach on the surface.

Pressure Coefficient Contours

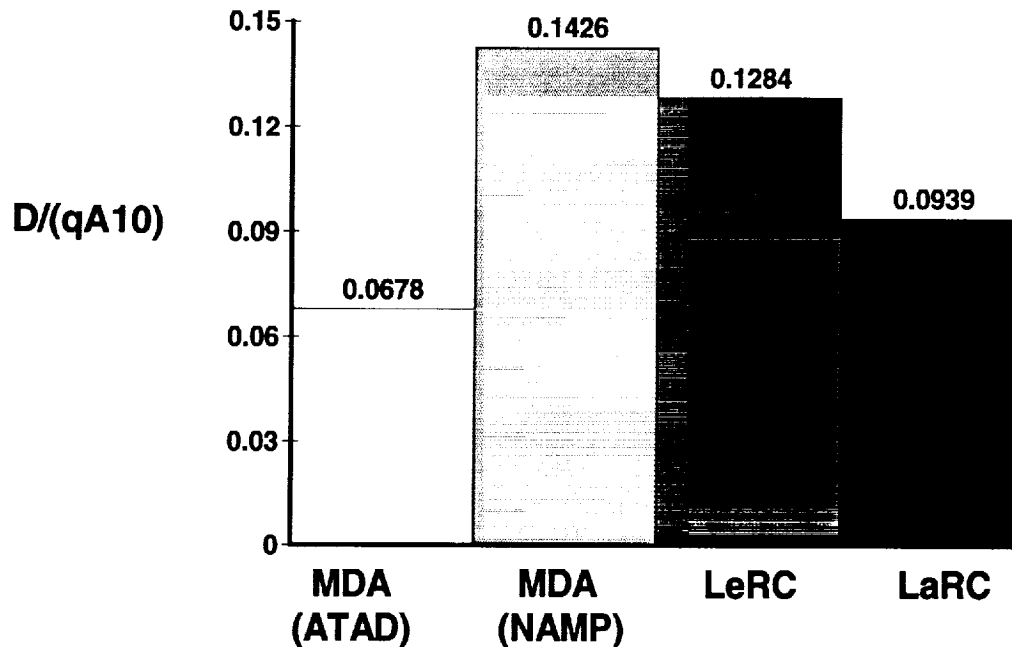
- 1605 Configuration, Mach 0.95 -



This figure shows the pressure contours and distribution as a function of non-dimensional flap length on the top nozzle flap surface for the 1605 configuration at Mach 0.95. Three different sections of the flap are presented on the pressure coefficient plot, with the $y/w=0.05$ representing the flap centerline. Examining the centerline curve shows that the pressure coefficient reflects the effect of the expansion wave at approximately $x/L=0.04$, and the significant separation above $x/L=0.16$. Pressure coefficient distributions for all CFD codes exhibited the same trends for the 1605 nozzle at Mach 0.95, with slight variations in shock/expansion wave location.

Comparison of 1605 CFD Data

- Mach 0.95 -

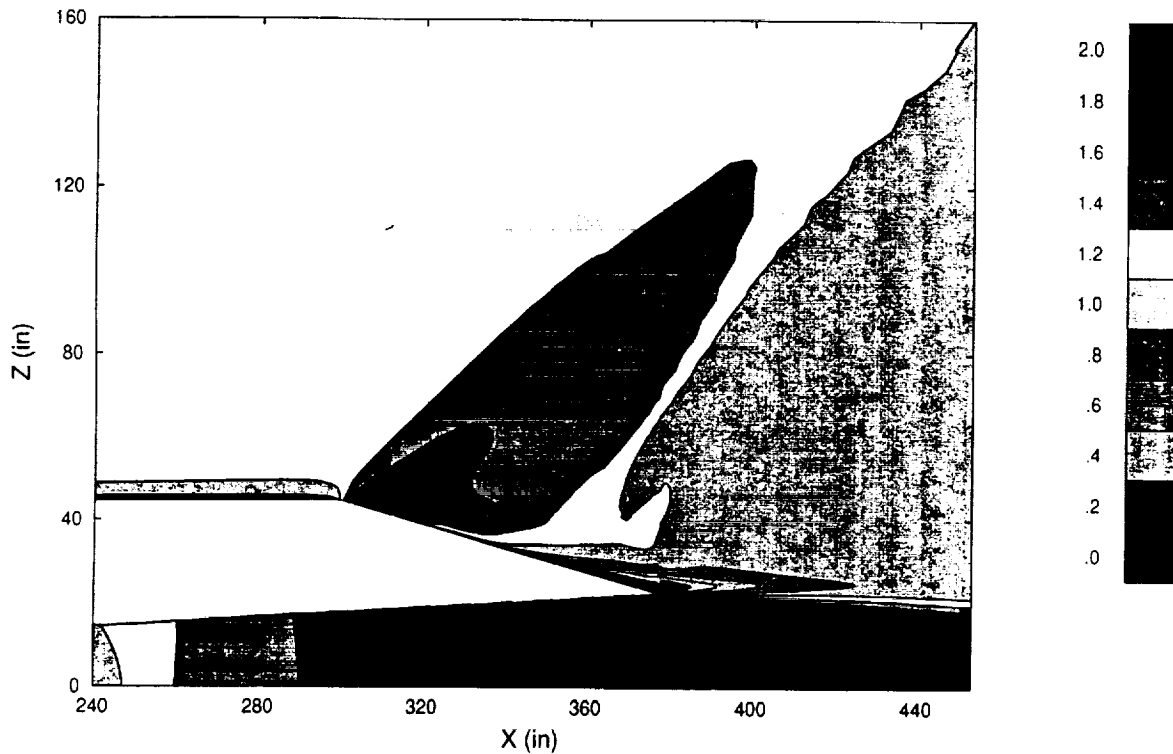


This figure shows the final drag coefficient results for the 1605 configuration at Mach 0.95. McDonnell Douglas results are represented by MDA-NAMP and MDA-ATAD, respectively. NASA Lewis and Langley results are represented by LeRC and LaRC, respectively. The Mach 0.95 case for the 1605 configuration yielded the largest discrepancies between team member results of all the test cases. Note that the MDA-NAMP and LeRC results are within 10%. This is good agreement considering the highly unstable nature of this separated flow problem. The problem is complicated by the fact that the problem is subsonic, sonic and supersonic along a streamline, and the fact that the codes must resolve exactly the location of the supersonic transition. Also, the agreement between MDA-NAMP and LeRC results is consistent with the AGARD validation results, which show nearly identical pressure coefficient distributions for the non-axisymmetric nozzle at the Mach 0.94 condition. For this Mach 0.95 case, the boattail drag coefficient likely lies in the ballpark of the MDA-NAMP and LeRC results.

The MDA-ATAD results for the 1605 configuration at Mach 0.95 should have been very close to the MDA-NAMP results due to the fact that the NASTD was the flow solver for both cases. However, MDA-ATAD computations at Mach 0.95 yield significantly lower pressure drag results than MDA-NAMP results. The MDA-ATAD solution of the 1605 configuration at Mach 0.95 encountered numerical convergence challenges that were attributable to the grid packing density in the vicinity of the nozzle boattail hinge line coupled with significant flow separation over the entire boattail surface. The consensus of the team is that the MDA-ATAD solutions significantly underpredict nozzle boattail drag at Mach 0.95, and should not be used.

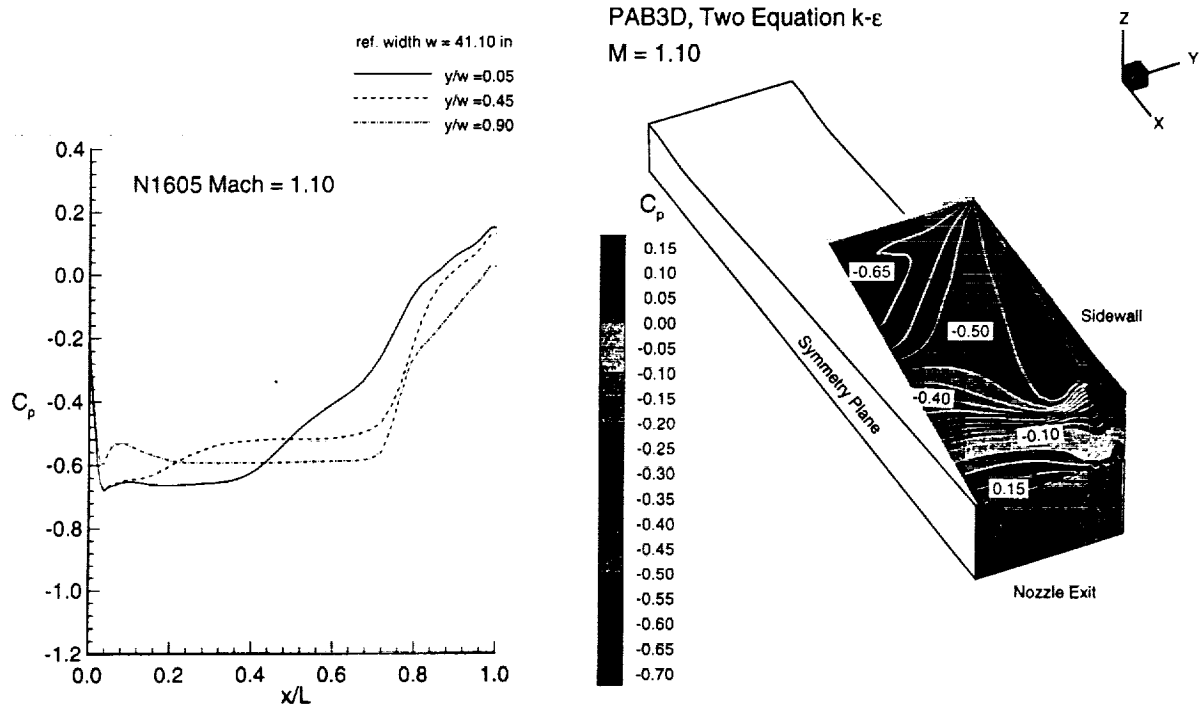
The LaRC results for the 1605 configuration at Mach 0.95 are approximately 30% lower than the MDA-NAMP and LeRC results. This is consistent with the results from the AGARD validation study for the B.4 nozzle at Mach 0.94.

Mach Number Contours Along Centerline - 1605 Configuration, Mach 1.1 -



This figure shows the Mach number contours along the centerline of the top flap of the 1605 nozzle at Mach 1.1. The flow is uniform prior to the nozzle hinge line, and begins to expand at the nozzle flap hinge line. For this case, the external flow expands around the nozzle boattail flap hinge and recompresses through a normal shock wave located at approximately the halfway point of the nozzle flap length. Separation from the afterbody surface occurs behind the normal shock wave, and the flow does not reattach on the surface. The flow separation is not as severe as the Mach 0.95 case was, and the solution for the Mach 1.1 case is not as challenging as the previous Mach 0.95 solution.

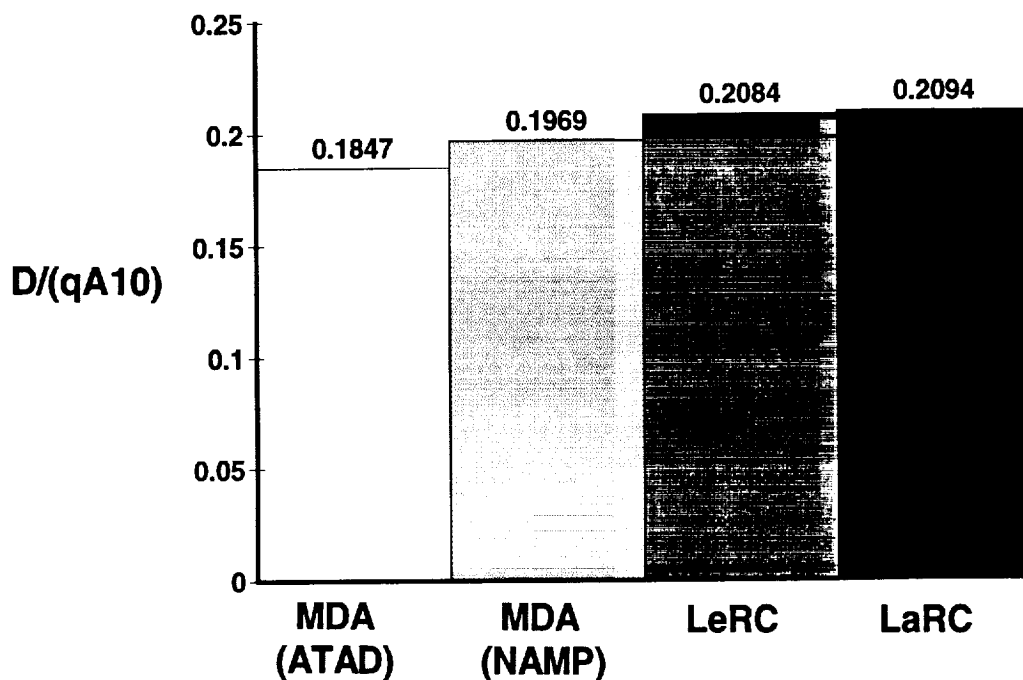
Pressure Coefficient Contours - 1605 Configuration, Mach 1.1 -



This figure shows the pressure contours and distribution as a function of non-dimensional flap length on the top nozzle flap surface for this configuration. Examining the centerline ($y/w=0.05$) curve on the pressure coefficient plot shows that the pressure coefficient reflects the effect of the expansion wave at approximately $x/L=0.04$, and the separation above $x/L=0.4$. Note that the pressure recovery is not as significant for this configuration, compared to the Mach 0.95 case, which indicates that the Mach 1.1 case has significantly less separation than the Mach 0.95 case. Pressure coefficient distributions for all CFD codes exhibited the same trends for the 1605 nozzle at Mach 1.1, with slight variations in shock/expansion wave location.

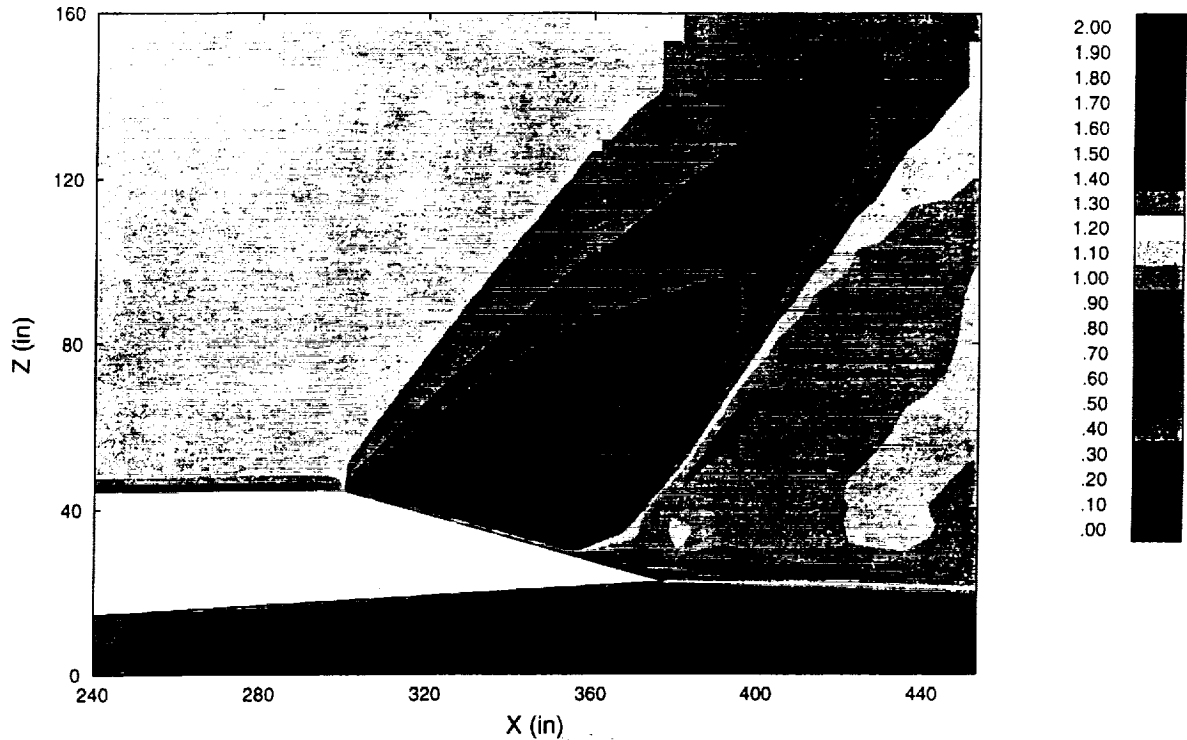
Comparison of 1605 CFD Data

- Mach 1.10 -



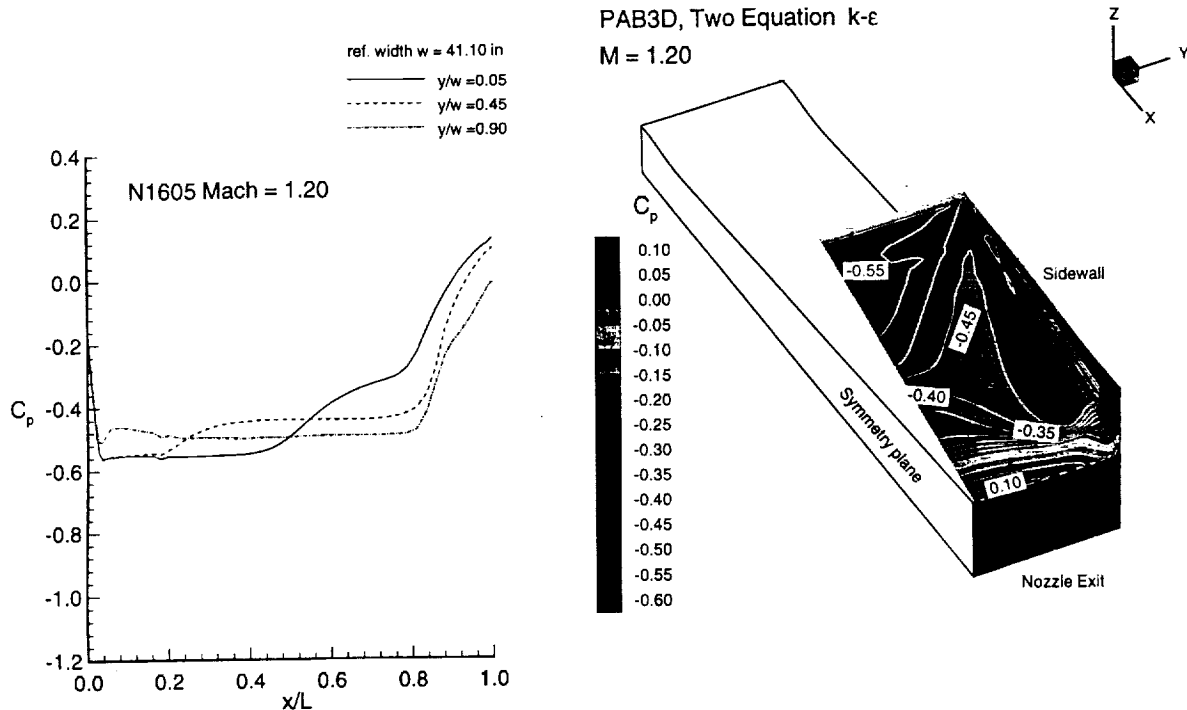
This figure shows the final drag coefficient results for the 1605 configuration at Mach 1.1. Because the separation for this case was less severe than the Mach 0.95 case, the CFD codes were better able to predict the flow characteristics, and the results were consistent. For example, the MDA-NAMP and NASA results agreed within 5%. Even more striking, the LeRC and LaRC results agreed within 0.5%. The MDA-ATAD results were approximately 10% lower than the MDA-NAMP results even though the grid was identical for both applications. The team chose to use the MDA-NAMP results due to the higher user experience level. For the Mach 1.1 case, the boattail drag coefficient could accurately be predicted as the average of the MDA-NAMP, LeRC and LaRC results.

Mach Number Contours Along Centerline - 1605 Configuration, Mach 1.2 -



This figure shows the Mach number contours along the centerline of the top flap of the 1605 nozzle at Mach 1.2. The flow is uniform prior to the nozzle hinge line, and begins to expand at the nozzle flap hinge line. For this case, the external flow expands around the nozzle boattail flap hinge line and recompresses through a normal shock wave located approximately three-quarters of the way down the nozzle flap length. Separation from the afterbody surface occurs behind the normal shock wave, and the flow does not reattach on the surface. The flow separation is less severe than the Mach 1.1 case, and therefore, the Mach 1.2 case is the most straightforward solution of the three Mach numbers studied.

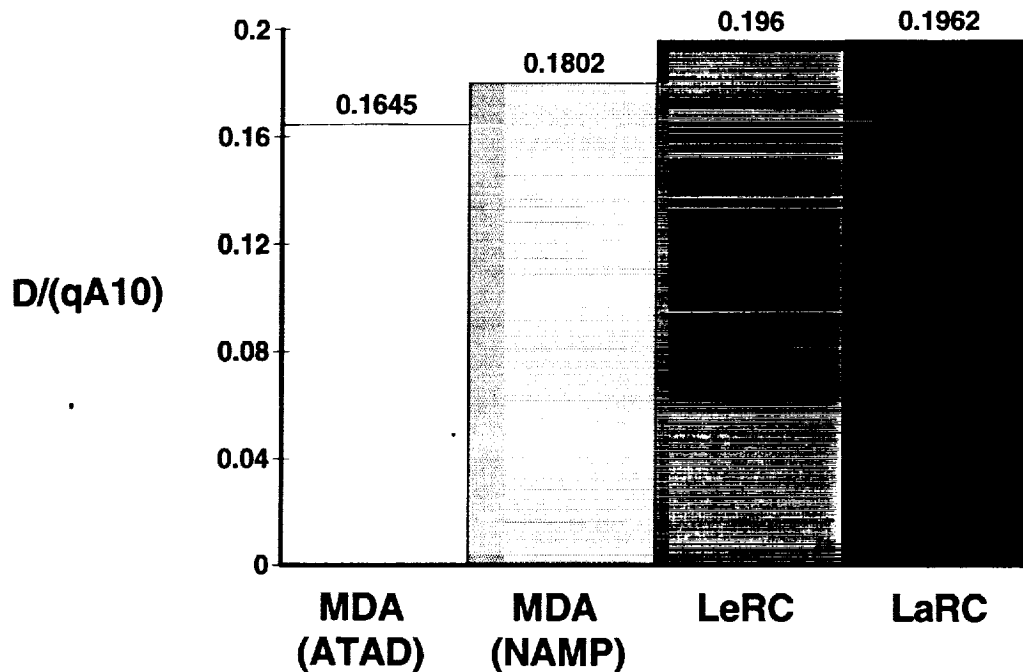
Pressure Coefficient Contours - 1605 Configuration, Mach 1.2 -



This figure shows the pressure contours and distribution as a function on non-dimensional flap length on the top nozzle flap surface for this configuration. Examining the centerline ($y/w=0.05$) curve on the pressure coefficient plot shows that the pressure coefficient reflects the effect of the expansion wave at approximately $x/L=0.04$, and the separation above $x/L=0.75$. Note that the pressure recovery is not as significant for this configuration, compared even to the Mach 1.1 case, which indicates that the Mach 1.2 case has significantly less separation than the Mach 1.1 case. Pressure coefficient distributions for all CFD codes exhibited the same trends for the 1605 nozzle at Mach 1.2, with slight variations in shock/expansion wave location.

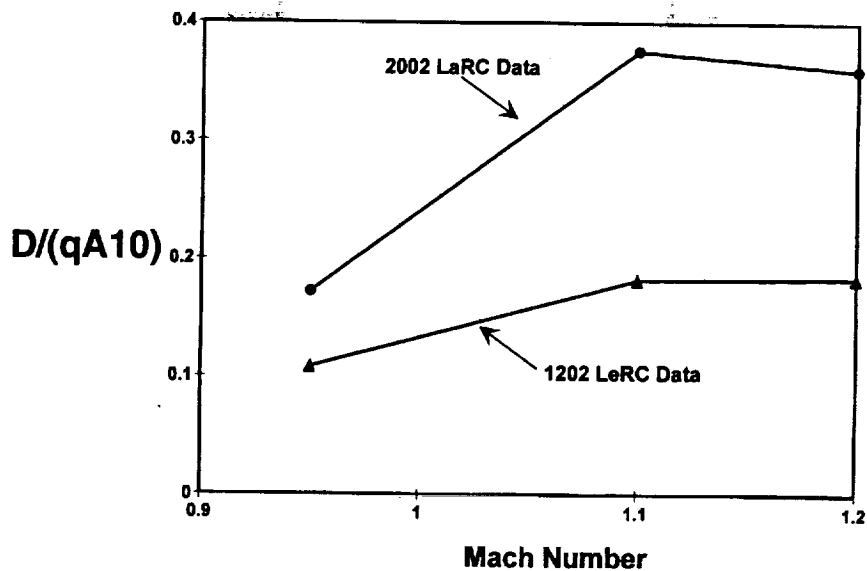
Comparison of 1605 CFD Data

- Mach 1.20 -



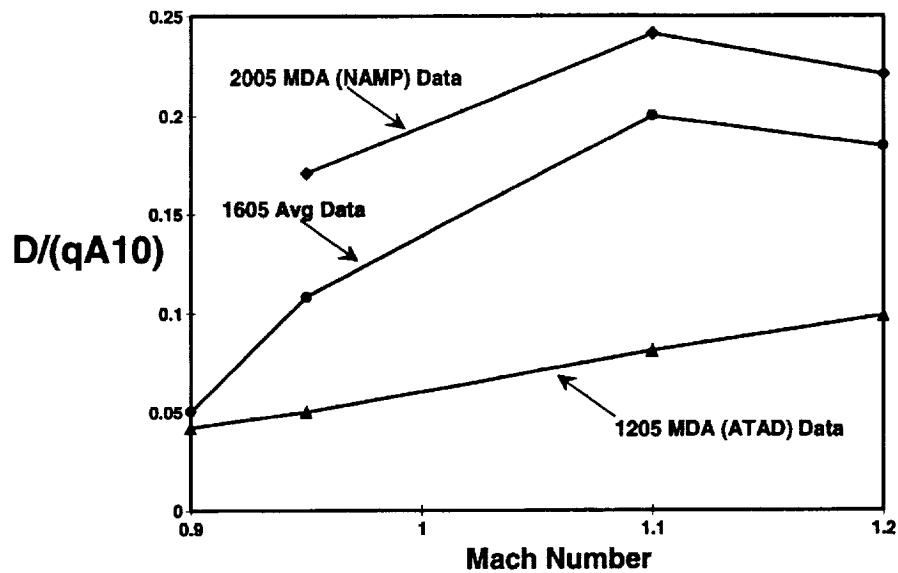
This figure shows the final drag coefficient results for the 1605 configuration at Mach 1.2. Because the separation for this case was less severe than the other cases, the CFD codes were able to predict consistent results. For example, MDA-NAMP and NASA results agreed within 8%. Once again, the LeRC and LaRC results were essentially identical. Again, the MDA-ATAD results were approximately 8% lower than the MDA-NAMP results even though the grid was identical for both applications. The team chose to use the MDA-NAMP results due to the higher user experience level. For the Mach 1.2 case, the boattail drag coefficient could accurately be predicted as the average of the MDA-NAMP, LeRC and LaRC results.

A9/A10 = 0.2 CFD Predictions



This figure shows nozzle boattail drag coefficient as a function of Mach number for the 0.2 area ratio solutions. LaRC was responsible for the 2002 solutions (top line) and LeRC was responsible for the 1202 solutions (bottom line). The 2002 solution at Mach 0.95 is probably underpredicted based on the AGARD validation study results presented earlier, and should be considered a ballpark estimate for this specific case. The 1202 solution at Mach 1.2 is suspicious because nozzle boattail drag coefficient should be lower at Mach 1.2 than at Mach 1.1. This same anomaly is evident for both 12 degree boattail angle configurations.

A9/A10 = 0.5 CFD Predictions



This figure shows the solutions for the 0.5 area ratio solutions. MDA-NAMP was responsible for the 2005 solutions (top line), while MDA-ATAD was responsible for the 1205 solutions (bottom line). Again, the 1205 solutions appear to be uniformly underpredicted, and should not be used as absolute values. The 1605 solutions (middle line) represent the average of MDA-E and LeRC solutions for Mach 0.95, and the average of MDA-NAMP, LeRC and LaRC solutions for Mach 1.1 and 1.2.

Comparison of CFD Results to 95 IMS Database

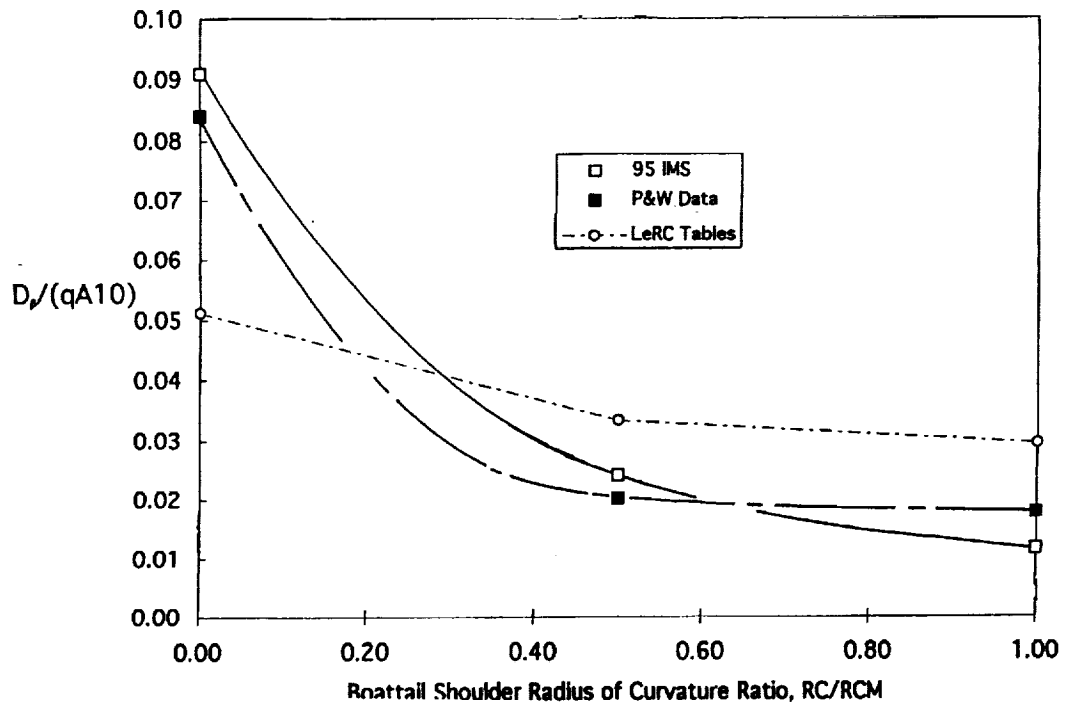
- o IMS Validation**
- o Mach 0.95, 1.1, and 1.2**

As described earlier, the CFD results were to be used to substantiate and enhance the concurrent IMS database update activity. Before comparisons between CFD and IMS are made, a brief comparison of IMS to experimental data will be discussed.

Comparison of Nozzle Drag Data w/Previous Method

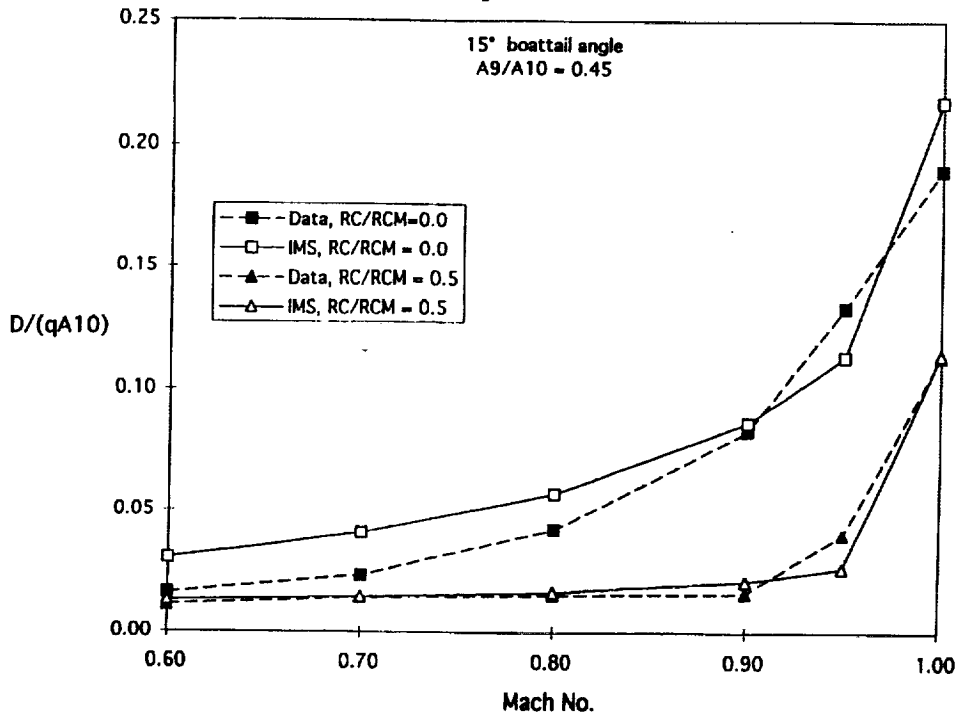
- 2D Nozzle, $A_9/A_{10}=0.25$, $\beta = 16$ deg -

$M = 0.9$



This figure shows a plot that was presented earlier comparing the previous boattail drag coefficient method with experimental data. It has been updated here by adding the new IMS database predictions. The IMS database values are shown as the line with the open symbols, and show excellent agreement with the non-axisymmetric experimental data for the entire range of radius of curvature ratio values.

Nozzle Drag Correlation, IMS vs Test **NASA TMX-1517** **Axisymmetric Nozzles**

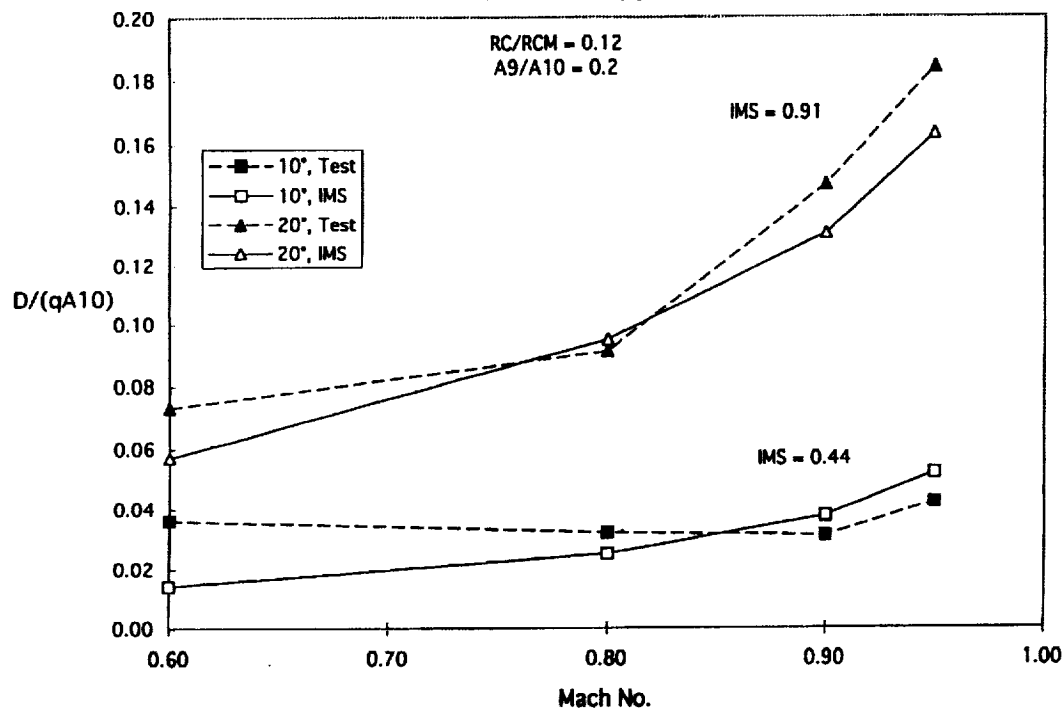


This figure shows a comparison of IMS predictions for an axisymmetric nozzle with a 15 degree boattail flap angle and an area ratio of 0.45. In this figure, the lines with darkened symbols represent the experimental data, while the lines with the open symbols represent the IMS predictions. The plot is nozzle boattail drag coefficient versus Mach number, and the IMS predictions agree without bias with the experimental data for two different radius of curvature ratios (0.0 and 0.5).

Nozzle Drag Correlation, IMS vs Test

NASA TP-3440

2D Nozzles

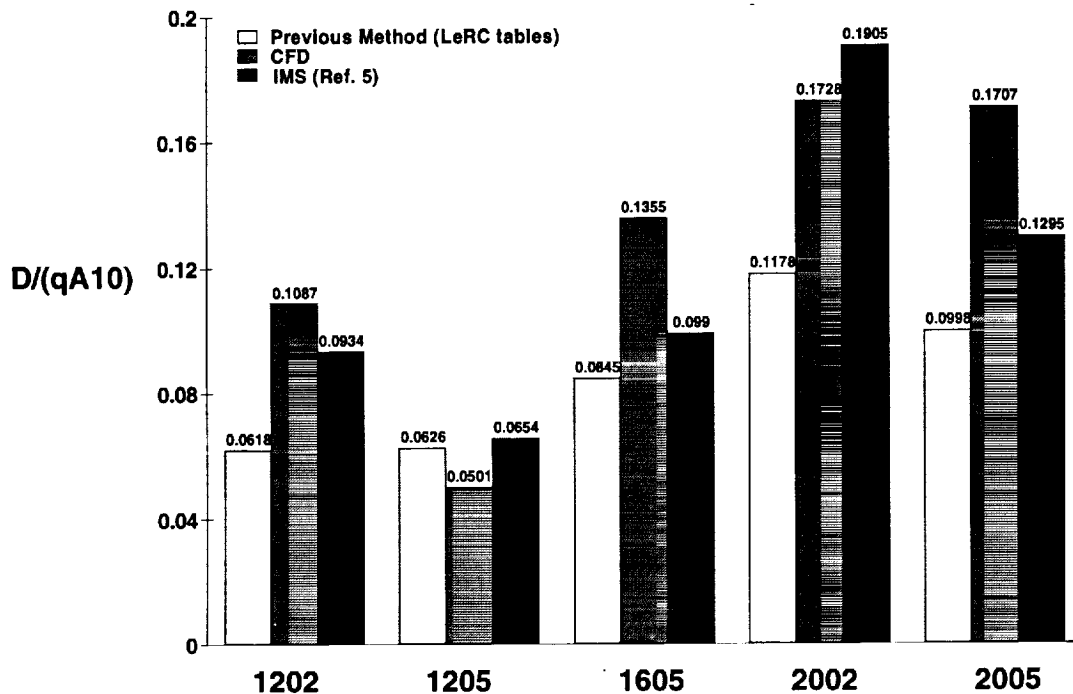


This figure shows a comparison of IMS predictions for a non-axisymmetric nozzle with a radius of curvature ratio of 0.12 and an area ratio of 0.2. Again, the experimental data is represented by the darkened symbols, while the IMS predictions are represented by the open symbols. The plot is nozzle boattail drag coefficient versus Mach number, and the IMS predictions agree without bias with the experimental data for two different boattail flap angles (10 and 20 degrees). Based on these comparisons and additional supporting information not shown explicitly here, it is clear that the IMS prediction method with the recently updated database accurately predicts axisymmetric and non-axisymmetric nozzle boattail drag coefficient for complex geometry nozzles. Comparison with CFD results on HSCT specific nozzles would fully substantiate this new methodology for the HSCT project.

Isolated Nozzle Boattail Drag Coefficient Prediction Comparison

- Referenced to A10

- Mach 0.95

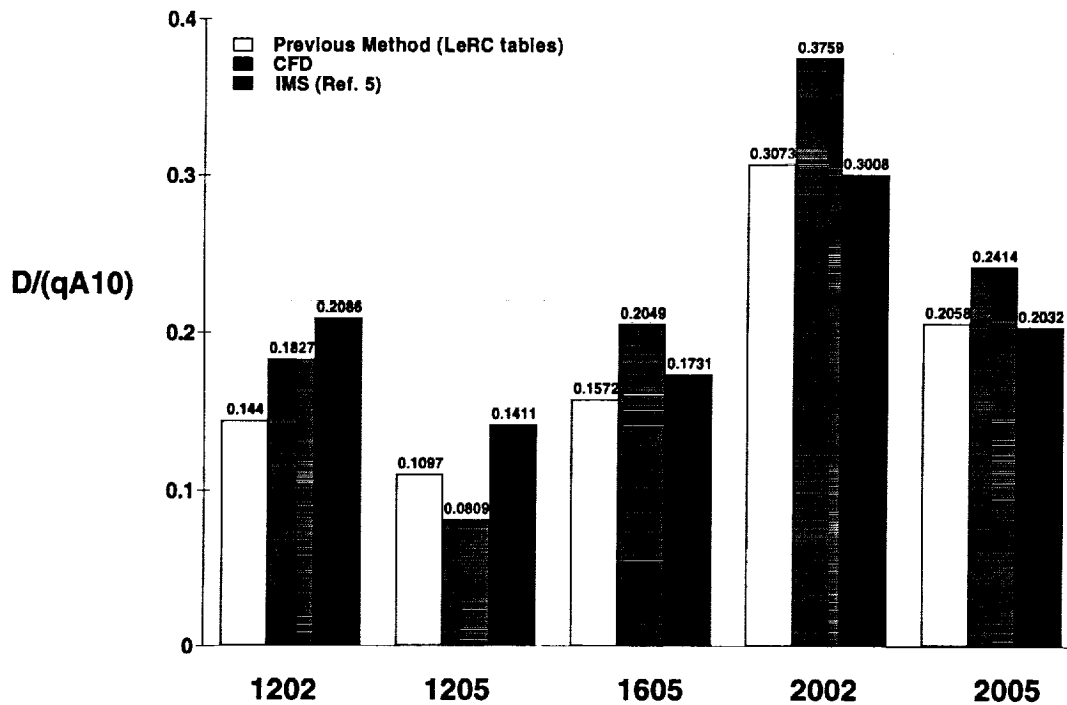


This figure shows a comparison of the IMS, CFD and previous method predictions at Mach 0.95. Each of the six geometry configurations are shown individually on the bar graph. In general, the IMS and CFD predictions generally agree within 10-15%, and there is no apparent bias or trend with boattail angle or area ratio. Due to the fact that the Mach 0.95 case was highly separated and difficult to obtain CFD solutions for, the CFD results in the figure should only be used to substantiate the IMS predictions. The previous method consistently underpredicts the IMS estimates by as much as 50%. No further conclusions can be drawn from this case.

Isolated Nozzle Boattail Drag Coefficient Prediction Comparison

- Referenced to A10

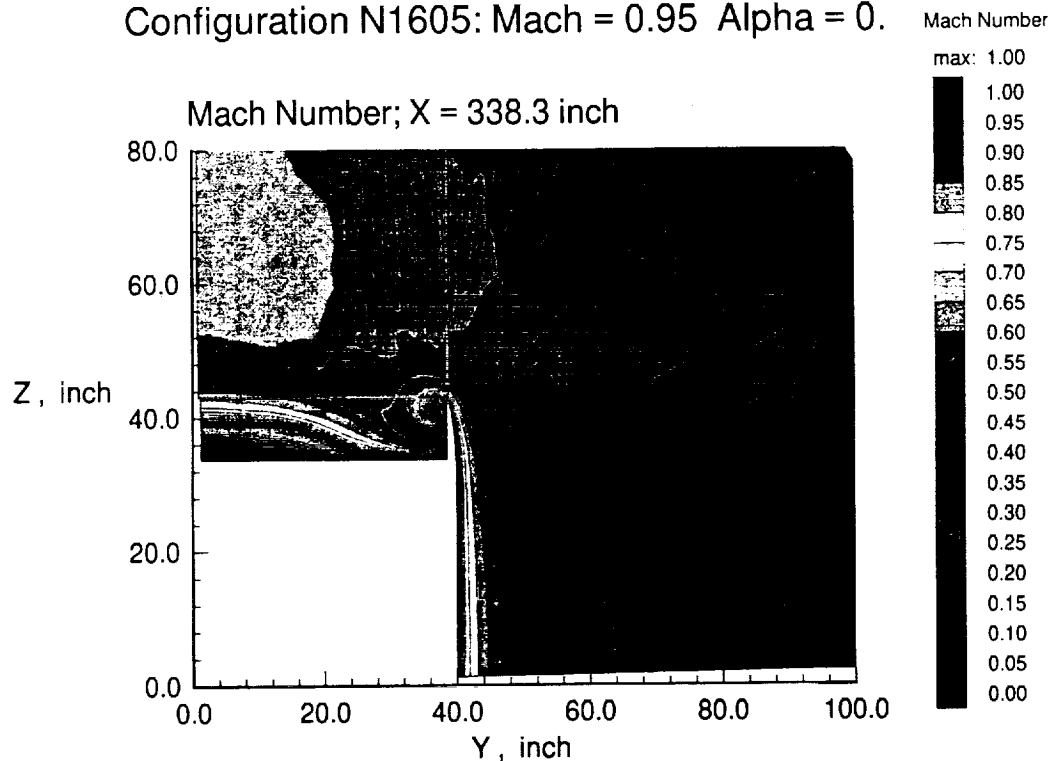
- Mach 1.10



This figure shows the same comparison at Mach 1.1. In general, the IMS and CFD predictions generally agree, but there is an apparent trend with boattail angle. At a 12 degree boattail angle, the IMS prediction is slightly higher than the CFD prediction for the area ratio of 0.2. At a 16 degree boattail angle, the predictions also agree very closely. At a 20 degree boattail angle, the CFD predictions are higher than the CFD predictions for both area ratios studied. It is likely that this trend is caused by sidewall effects, and is discussed in detail later. The previous method consistently underpredicts the IMS estimates for boattail angles less than 20 degrees. For the 20 degree boattail angle cases, the previous method and the IMS predictions agree within 1%, but both represent estimates for nozzles without sidewalls.

Isolated Nacelle Drag Study: Flow Cross Section

Configuration N1605: Mach = 0.95 Alpha = 0.

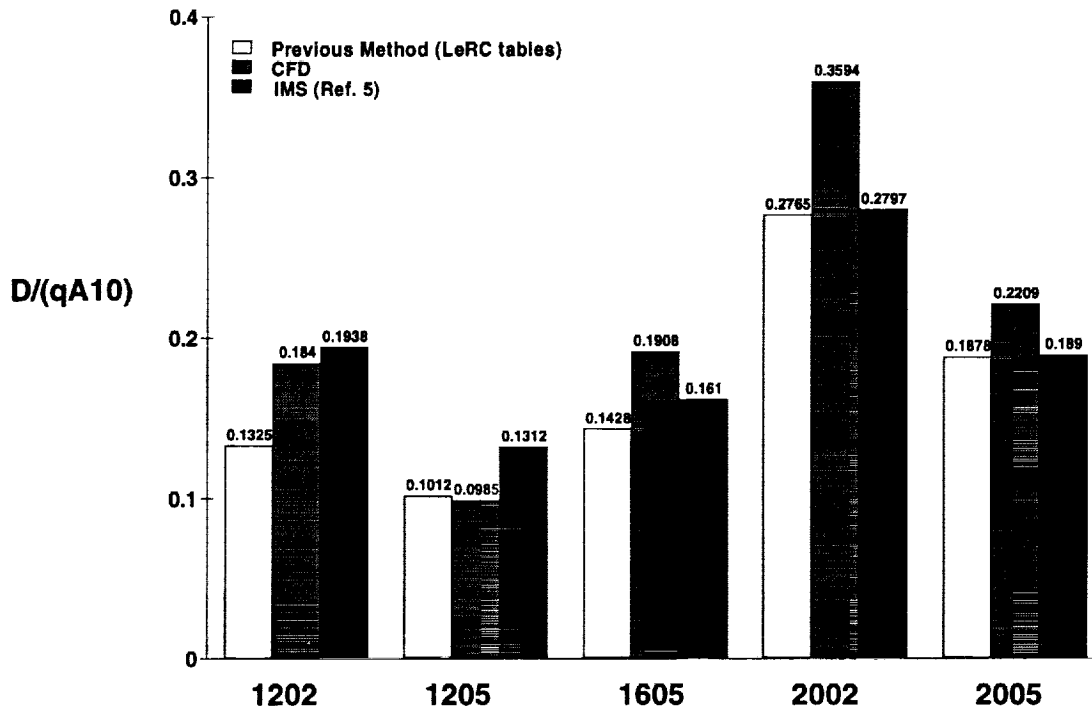


The IMS and previous method predictions are based on non-axisymmetric nozzles without sidewalls. The CFD predictions use the DSM nozzle, which does have sidewalls. Based on the results of the CFD studies, the sidewalls on a non-axisymmetric nozzle cause a decrease in the pressure relief from the top of the nozzle flap to the ambient flow due to end-plating and vortex trapping effects, and thus may cause an increase in drag coefficient. An example of this flow phenomena is shown in the figure, which depicts an aft facing forward view of the DSM nozzle. Higher pressure ambient flow is shown rolling over the top of the sidewall and pressurizing the top of the nozzle boattail flap. If the sidewall is removed, the pressurizing of the flap may increase, and the boattail drag coefficient may be reduced. One possible explanation of the trend shown in the previous figure is that as boattail angle increases, the effect of the sidewall on the boattail flap increases. At 12 degrees, the sidewall does not significantly impact the pressurization of the nozzle boattail flap. However, at 16 and 20 degrees boattail angle, the effect of the sidewall may significantly impact the prediction of nozzle boattail drag coefficient. A follow-on study is underway to update the IMS database for sidewall effects. Also, an on-going CFD study will evaluate the delta nozzle boattail drag coefficient due to removing the sidewalls using various configurations evaluated in this study.

Isolated Nozzle Boattail Drag Coefficient Prediction Comparison

- Referenced to A10

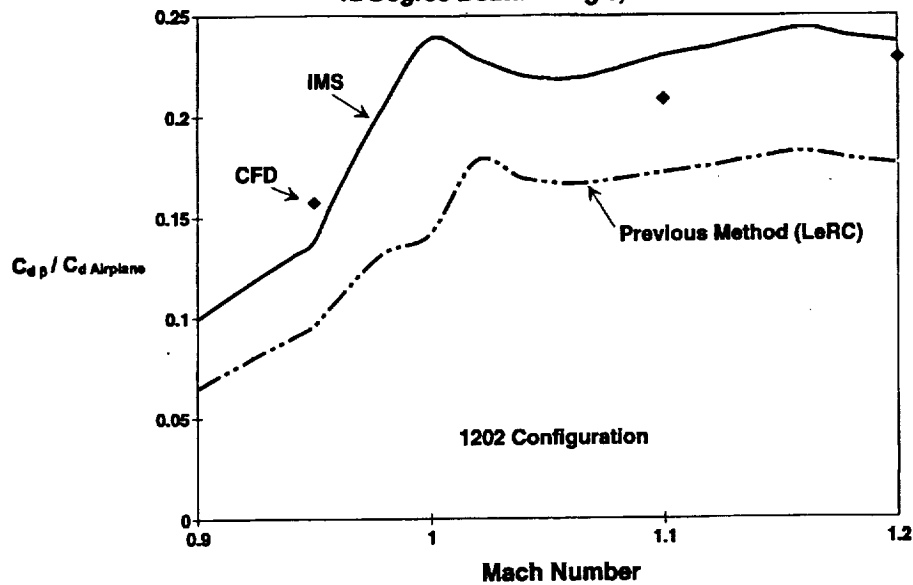
- Mach 1.20



This figure shows the same comparison at Mach 1.2. In general, the IMS and CFD predictions generally agree. Again, there is an apparent trend with boattail angle, and the conclusion is the same as for the Mach 1.1 case. The sidewalls appear to affect the 16 and 20 degree boattail angle CFD predictions. In addition, the previous method underpredicts IMS estimates for boattail angles less than 20 degrees, which is consistent with the Mach 1.1 results. Like the Mach 1.1 results, the previous method and IMS estimates agree closely for the 20 degree boattail angle cases.

Comparison of CFD, IMS and Previous Method Drag Ratios

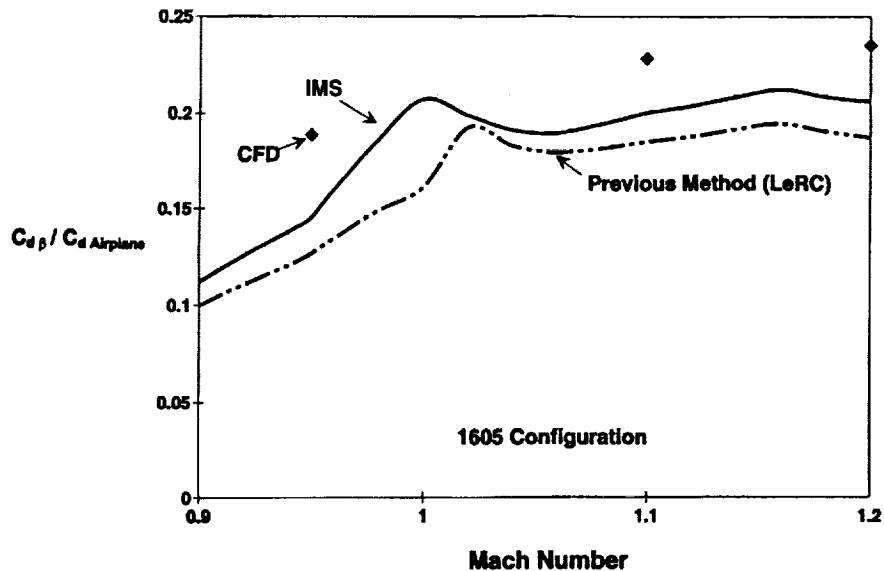
- Ratio of Boattail Drag Coefficient to Aircraft Total Drag Coefficient
- Referenced to Aircraft Wing Area
- 12 Degree Boattail Angle, $A_9/A_{10} = 0.187$



This figure shows a comparison of CFD, IMS and previous method nozzle drag coefficient predictions normalized with total HSCT airplane drag coefficient for the 1202 configuration. All drag coefficients are referenced to the airplane wing area for this comparison, and the total airplane drag coefficient includes the nozzle boattail drag element. For the 1202 configuration, the CFD and IMS predictions are of the same magnitude, and this substantiated that the previous method significantly underpredicts nozzle boattail drag coefficient. The previous method predicts that nozzle boattail drag accounts for approximately 15% of the total airplane drag above Mach 1.0, while the CFD and IMS predict that nozzle boattail drag accounts for 20-25% of the total airplane drag above Mach 1.0. Because the HSCT nozzle would likely operate at transonic boattail angles of approximately 12 degrees, the more accurate CFD and IMS predictions would significantly affect the aircraft transonic performance, and thus would impact the airplane sizing and mission performance.

Comparison of CFD, IMS and Previous Method Drag Ratios

- Ratio of Boattail Drag Coefficient to Aircraft Total Drag Coefficient
- Referenced to Aircraft Wing Area
- 16 Degree Boattail Angle, $A_9/A_{10} = 0.467$



This figure shows the same comparison for the 1605 configuration. The CFD predictions are consistently larger than the IMS predictions for this case primarily because of the sidewall effects discussed earlier. However, the previous method underpredicts nozzle boattail drag for this configuration, and the replacement of the previous method with the IMS prediction methodology yields a method that is more applicable to the HSCT nozzle trade studies because of the updated nozzle drag coefficient database and additional nozzle geometrical flexibility. On average, the IMS method predicts 15-20% higher boattail drag for this configuration than the previous method.

Lessons Learned

- o **CFD Grids Must Be:**
 - **Generated by One Organization**
 - **Thoroughly Checked Out Prior to Production Runs**
- o **Multiple CFD Flow Solvers Can Be Used to Compute a Matrix of Solutions**
 - **AGARD17 Validation Check**
 - **Common Configuration Test Case**
 - **Resources**
- o **Configurations With Freestream Mach Numbers Close to 1.0 (0.95) and Large Boattail Angles Pose Serious Challenges and Limitations**
 - **Current CFD Codes**
 - **Current Turbulence Models (Affects Shock Position and Pressure Recovery)**
 - **Solutions Grid Dependent**
- o **Required 1 Month (Calendar Time) Per Case for Final Results**
- o **BI-Weekly Telecons, and Goal-Oriented Schedule Resulted in Focused Program and Provided Timely Results**

The most significant lesson learned is that multiple CFD flow solvers can be used to compute results for a matrix of configurations. In this case, multiple flow solvers were used by multiple team members located throughout the country. The key to a successful program using this team approach involves setting up a stringent validation process. Prior to solving HSCT specific configurations, each flow solver was required to solve an established configuration (AGARD) with proven experimental data. Upon completion of this exercise, each team member was required to analyze the baseline configuration. The program did not begin in earnest until all team members agreed on the results from analyzing the baseline configuration. This strategy worked well for this team, and proved that multiple CFD flow solvers can be used. The major benefit of this strategy is that it spreads the computational resource requirements throughout the team, and reduces the overall time required for the entire program.

In order to minimize differences in the results between flow solvers, the inputs must be kept as standardized as possible. In general, that means using the same grids and the same type of turbulence model. The CFD grids should all be generated by the same organization, and should be thoroughly checked out using one of the flow solvers prior to distribution to the rest of the team. Small changes can be made to the grids by each team member to better suit their respective flow solver, but these changes should be kept to a minimum to reduce the possibility of grid dependent differences in the solutions. Also, similar turbulence models should be used to ensure that result differences do not stem from the difference in turbulence models. This effect could be significant for highly separated configurations.

Configurations with freestream Mach numbers close to 1.0, and large boattail angles pose serious challenges and limitations. Current CFD codes and turbulence models have difficulty solving equations when Mach number approaches unity, and this affects shock position and pressure recovery. Thus, solutions to these types of configurations tend to be grid dependent.

Summary

- o Previous Boattail Drag Method Inadequate**
- o IMS Method w/CFD Validation Preferred Method**
 - Update Database Using Non-Axi Test Data**
 - In Place by March 1995 for Use in Nozzle Downselect Studies**
- o CFD Codes Validated with AGARD 17 Nozzle Test Data**
- o Full Scale 3765-100 MFTF Nacelle Configuration Used**
- o 27 CFD Cases Run, (Approx. 1.5 Million Points Each)**
- o Pressure Drag on Boattail Computed for All Cases**
- o All CFD Cases Successfully Completed Prior to Commencement of Nozzle Downselect Studies**

Nozzle boattail drag is significant for the HSCT and can be as high as 25% of the overall propulsion system thrust at transonic conditions. Thus, nozzle boattail drag has the potential to create a thrust-drag pinch and can reduce HSCT aircraft aerodynamic efficiencies at transonic operating conditions. In order to accurately predict HSCT performance, it is imperative that nozzle boattail drag be accurately predicted.

Previous methods to predict HSCT nozzle boattail drag were suspect in the transonic regime. In addition, previous prediction methods were unable to account for complex nozzle geometry and were not flexible enough for engine cycle trade studies. A computational fluid dynamics (CFD) effort was conducted by NASA and McDonnell Douglas to evaluate the magnitude and characteristics of HSCT nozzle boattail drag at transonic conditions. A team of engineers used various CFD codes and provided consistent, accurate boattail drag coefficient predictions for a family of HSCT nozzle configurations. The CFD results were incorporated into a nozzle drag database that encompassed the entire HSCT flight regime and provided the basis for an accurate and flexible prediction methodology.

Four teams of analysts were involved in the CFD study: NASA-Lewis Research Center, NASA Langley Research Center, and McDonnell Douglas Aerospace. Three CFD flow solvers were used, and were validated using Advisory Group for Aerospace Research and Development (AGARD) data, and a baseline HSCT nozzle configuration. Once the CFD codes were validated, the matrix of nozzle configurations were defined and predictions of nozzle boattail drag were generated. Each configuration studied incorporated a 3765 mixed flow turbofan and an axisymmetric inlet. 27 total CFD cases were run, and each case was comprised of approximately 1.5 million data points. Pressure drag on the boattail surfaces was computed and nozzle boattail drag coefficient was generated via a post-processed pressure integration. All CFD cases were successfully completed in a timely fashion.

Conclusions

- o **CFD Solutions Grid Dependent for Mach 0.95, Large Boattail Angle Cases**
 - **Significant Separation**
 - **Large Variation In CFD Results Between Teams**
- o **CFD Solutions at Mach 1.1 & 1.2 Well Defined**
 - **Good Agreement Between Teams**
- o **CFD Substantiates IMS Transonic Predictions**
 - **Part of IMS vs CFD Cd Difference Due to Sidewall Effect**
 - o **IMS Underpredicts at Boattail Angles > 16 deg**
 - **IMS Overpredicts for 12 deg Boattail Angle Cases**
 - **Transonic Wind Tunnel Data Required to Quantify Sidewall Fence Effect**
- o **CFD Accurately Predicts Isolated Nozzle Boattail Pressure Profiles**
 - **Consistent Results Using 3 Different Codes**

The CFD solutions were grid dependent for the Mach 0.95, large boattail angle cases. These cases experienced significant separation, and resulted in a large variation (30%) between team results for the baseline configuration. The CFD results at Mach 1.1 and 1.2 were well defined, and there was excellent agreement between the team results. NASA LeRC and LaRC agreed within 1% for these cases. The CFD and IMS method results at Mach 0.95 generally agreed within 30%, but no clear bias was apparent in the comparison. Therefore, the Mach 0.95 CFD results were only used to substantiate the approximate magnitude of the IMS predictions at Mach 0.95. The Mach 1.1 and 1.2 CFD results were generally within 20% of the IMS predictions, but showed a bias that could have been caused by the DSM nozzle sidewalls. The CFD predictions included nozzle sidewalls, while the IMS database did not include sidewalls. Because of this difference, the CFD predicted slightly higher nozzle drag coefficients for higher boattail angle cases (16 and 20 degrees), and this was consistent with the expected sidewall flow effect. Future work with CFD will quantify the sidewall effect, and incorporate this effect into the IMS database. For the Mach 1.1 and 1.2 cases, the CFD results substantiated the magnitude of the IMS predictions, and were incorporated as part of the nozzle drag coefficient database for use in future HSCT propulsion system performance calculations.

For this study, the CFD flow solvers accurately predicted isolated nozzle boattail pressure profiles and boattail drag coefficients. Consistent results were obtained using three different flow solvers. The results corroborated with the IMS database and provided a more applicable method for accurate prediction of transonic HSCT nozzle boattail drag.

ACKNOWLEDGMENTS

The authors wish to thank the following team members for their dedicated effort. The success of this study is directly related to the excellent quality of the results generated by the following personnel; Nick Georgiadis, Fred Smith and Joe Holcomb of NASA Lewis Research Center; Khaled Abdol-Hamid, John Carlson, and Peter Coen of NASA Langley Research Center; Ray Cosner, Chris Culbertson, Greg Finfrock, Jay Jones, Rob Jonietz, Walt LaBozzetta, Bill Regnier and Hoyt Wallace of McDonnell Douglas Aerospace.

REFERENCES

1. Silhan, F.V., and Cabbage, J.M., "Drag of Conical and Circular-Arc Boattail Afterbodies at Mach Numbers from 0.6 to 1.3", NACA Research Memorandum RM L56K22, January 1957.
2. Bangert, L.S., and Carson, G.T. Jr., "Effect of Afterbody Geometry on Aerodynamic Characteristics of Isolated Nonaxisymmetric Afterbodies at Transonic Mach Numbers", NASA Technical Paper TP 3236, September 1992.
3. Stevens, H.L., Thayer, E.B., and Fullerton, J.F., "Development of the Multi-Function 2-D/C-D Nozzle", AIAA Paper 81-1491, July 1981.
4. Wallace, H.W., Hiley, P.E., Reinsberg, J.G., and Booher, M.E., "Advanced Nozzle Concepts Program Final Report; Summary of Results and Nozzle Integration Design Criteria", AFWAL-TR-81-3165, Volume I, January 1982.
5. Wallace, H.W., "Nozzle Boattail Drag Topics", Presentation (unpublished) to the Propulsion System Evaluation Team of the NASA Lewis Research Center Critical Propulsion System Components Program, St. Louis, MO, March 1995.
6. Cooper, K., "NPARC 2.0 Features and Capabilities", AIAA 95-2609, Presented at the 31st Joint Propulsion Conference, July 10-12, 1995.
7. Abdol-Hamid, K.S., Carlson, J.R., and Lakshmanan, B., "Application of Navier-Stokes Code PAB3D to Attached and Separated Flows with a $k-\epsilon$ Turbulence Model", NASA Technical Paper TP 3840, 1994.
8. Bush, R. H., "A Three-Dimensional, Zonal, Navier-Stokes Code for Subsonic Through Hypersonic Propulsion Flow Fields", AIAA 88-2830, Presented at the 24th Joint Propulsion Conference, July 1988.
9. AGARD Fluid Dynamics Panel (Working Group #17): Aerodynamics of 3D Aircraft Afterbodies, AGARD Advisory Report AR-318, September, 1995.
10. Carlson, J.R., Pao, S.P., Abdol-Hamid, K.S., and Jones, W.T., "Aerodynamic Performance Predictions of Single and Twin-Jet Afterbodies", AIAA 95-2622, Presented at 31st Joint Propulsion Conference, July 1995.
11. Compton, W.B. III, Abdol-Hamid, K.S., and Abeyounis, W.K., "Comparison of Algebraic Turbulence Models for Afterbody Flow with Jet Exhaust", AIAA Journal, Volume 30, pp. 2716-2722, November 1992.
12. DeBonis, James R., Georgiadis, Nicholas J., Smith, Crawford F., "Validation of the NPARC Code for Nozzle Afterbody Flows at Transonic Speeds", NASA Technical Memorandum 106971, Presented at the 31st Joint Propulsion Conference, July 10-12, 1995.
13. Cosner, R.R., "CFD Validation Requirements for Technology Transition", AIAA 95-2227, Presented at 26th AIAA Fluid Dynamics Conference, June 19-22, 1995.
14. Shrewsbury, G.D., "Effect of Boattail Juncture Shape on Pressure Drag Coefficients of Isolated Afterbodies", NASA TM X-1517, March 1968.
15. Carlson, J.R., and Asbury, S.C., "Two-Dimensional Converging-Diverging Rippled Nozzles at Transonic Speeds", NASA Technical Paper TP 3440, July 1994.